Manuscript response file for ESSD-2024-335 "High resolution continuous flow analysis impurity data from the Mount Brown South ice core, East Antarctica"

Included in this file:

- (1) Overview of changes made to manuscript.
- (2) Comments from referees in black text.
- (3) Author's response (as a point-by-point reply to referee comments, as provided in the discussion stage of the submission, included here in *blue italicized text*).
- (4) Author's changes in manuscript (in *red italicized text* following the author responses. Additional changed made to the text described following the reply to reviewers).
- (5) Tracked-changes document produced using latexdiff.

Overview of major changes made to manuscript:

- Changes made to manuscript in response to referee comments, as described below in point-by-point reply to reviewers.
- Some sections of the manuscript have been re-arranged for clarity and readability of the manuscript mainly in the introduction. This is reflected in the tracked-changes document.
- A table has been added (now Table 1) with the delay time for each analyte measured from the standards.
- The order of what are now Tables 2 and 3 have been swapped so that they match the order in which they are referenced in the text.
- In a final inspection of the full dataset, the flowmeter data from the final run was found to be faulty, impacting only the insoluble microparticle data below approximately 85 m depth. This data has been removed from the published dataset as well as Figure 5 as we are not able to confirm its accuracy.
- MATLAB data calibration script has been included as a supplementary file.

Author comments:

We thank the reviewer for taking the time review the manuscript and provide thoughtful and constructive feedback. Reviewer comments and suggestions have been addressed; please see the below replies in blue italicized text.

Changes made to the revised manuscript in red italicized text.

Reply to RC1 (Tobias Erhardt):

Harlan et al. present a description of the measurement setup for the MBS CFA record and the associated uncertainties. Overall I found the manuscript to be complete, well written and very readable!

We thank the reviewer for the thoughtful feedback.

I only have some minor remarks that the authors should address before publication:

The most important one is a potential issue with the relative delay estimation between the two parameters (Section 4.4): The authors determine the signal delays using the maximum of the derivative during the transition into the standard measurements. This approach is certainly valid, but a small detail is missing from the discussion: The influence of the signal smoothing on this way of determining the relative signal delays. For higher signal smoothing the maximum of the derivative will occur systematically later as the derivative will have its maximum at approximately halve the signal amplitude. This will introduce a slight systematic overestimation of the signal delay for parameters with larger smoothing relative to parameters with less signal smoothing. I would encourage the authors to add a few sentences in this regard.

We thank the reviewer for bringing this up - we agree that this is an important point and well raised. We chose this method due to its ability to be applied to each run in a systematic way but agree that (as with all approaches) there is a certain degree of bias dependent on signal smoothing inherent to this method. We will text to address this:

"Other choices for delay calculations could have been to use the start of the rise or even the end of the rise, however due to smoothing can be hard to reliably identify, whereas the maximum of the derivative of the increase is easily and systematically identified. However, we recognize that this can introduce a minor offset between methods that are highly smoothed in comparison to those that have faster response times."

Changes made in manuscript: Text added in section "Signal delay time," (lines 254-257) as described above.

The second is the description of the differences between the 2018 and 2019 setups. Judging from the flow diagrams in Figure 3, the systems were quite different with respect to the parameters presented here. I would suggest the authors expand this section significantly to delineate all the differences also in terms of procedures.

We agree that more detail could be warranted by other CFA users/readers, especially with regards to run procedures. The most meaningful differences in the two system setups are described in the manuscript, namely the depth registration types i.e. the difference between using an encoder and a laser. We see the point raised that the two instruments/methods could influence the final depths slightly differently, however these effect of these differences on the final dataset are likely very minor. Some of the potential differences between the two methods include the shorter "dead time" with the laser vs the cable encoder, which must be fully removed and

replaced during frame changeover. Additionally, while the 55 cm piece lengths used in the 2018 campaign introduce more potential contamination at breaks, they make absolute depths more certain, as the top depths are known at every 55 cm rather than every meter. We will add a few more lines regarding that in the section titled "Depth scale".

Besides these depth differences, the systems were not in fact too different in the end (i.e. delay time to the conductivity measurement was in both systems 15 seconds (stated in section 4.4). Calibrations and processing of calibrations were made based on the same concentration and dilution of standards, following the same calibration data processing method. In section sampling resolution we explain how the different melt-rates influenced the resolution "These melt-rates produce a direct sampling resolution (independent of smoothing due to response time) of 0.58 and 0.68 mm, respectively"

We will add text to the methods sections specifically delineating the elements of the systems and procedures that were the same and/or different, elaborating on the system diagrams in Figure 3.

New section added "2.3 Primary differences between 2018 and 2019 CFA setups" on what is now page 8. This section details the most significant changes that were made to the system, and describes the anticipated impact of these changes on the data quality (lines 165-190).

Specific remarks:

L 123: "temperamental" is an odd choice of words. To avoid personification maybe describe in terms of noise sensitivity

We will update the text with more appropriate terms such as 'inconsistent' or 'erratic'.

The proposed change has been made in revised manuscript.

Section 3.0.2: See comment above.

Section 4.4: See comment above.

Section 5.0.1: Explain target meltrate especially in light of the density change downcore.

While we present here the melt-rate throughout each measurement campaign, during the 2018 campaign (top ~95 m), the melt-rate did in fact decrease as the firn/ice density increased downcore. We will elaborate further on this in section 5.0.1 to provide more clarity on how the melt-rate was adapted to the density changes.

Further detail on meltrate changes with respect to firn densification downcore have been added to section 4.1 (page 11).

Section 6.1: What makes the pH measurements more sensitive to the pressure fluctuations than the Na channel? From my understanding both are absorption spectroscopic methods and are thus more sensitive to mixing ratio fluctuations than the fluorescence detection.

Indeed both absorption methods are more sensitive than fluorescence methods. The acid method however is even more sensitive than the sodium method, because rather than being a "true" absorption method it relies on pH dye changes using a combination of two dyes to cover the full range of pH expected in ice core waters One could thus think of it as a double "absorption"

function, the dyes are each most efficient at one wavelength, but do impact each others max wavelength. The method is optimized and described in Kjær et al. (2016) so we refer to that for more details. Because the method is very sensitive to the dye to sample ratio, small flow changes (i.e. squeezing and wear of pump tubing, which naturally happens over time, as well as pressure changes and temperature changes) influence the method more than the also sensitive Na+ method. In the Na+ method, the issue (more so than exact mixing of reagent and standards) seems to be due to wear out of the IMER column over time, causing a slower drift. We refer to Kaufmann et al. (2008) for more information on that method.

Section 6.5: Please explain the filtering approach detailed enough so that others are able to replicate the same thing, if needed. This will also help to judge the imprint of the filter on the final dataset in terms of its frequency content.

We state in section 6.5 that the filtering approach was "applying a filter that applies a threshold cutoff to the differential of the signal (due to the characteristics of these features)." We agree that this could use more detailed elaboration. Text will be added to the manuscript which more explicitly describes the method of data filtering, stating text along the lines of the following:

"The passage of air bubbles through the detectors results in a signal characterized by a significantly steeper increase (and subsequent decrease) in the signal voltage than anything produced by variability in the ice core sample. Because of this characteristic peak shape, we are able to define for the differential of the dataset, a threshold, values above which we use to define "bubble spikes" in the data, which can be safely removed from the dataset."

Text has been added to section 5.5 to further explain the filtering approach used for data cleaning (lines 342-345).

References:

Kaufmann, P., Federer, U., Hutterli, M. A., Bigler, M., Schüpbach, S., Ruth, U., Schmitt, J., and Stocker, T. F.: An improved continuous flow analysis system for high-resolution field measurements on ice cores, Environmental Science & Technology, 42, 8044–8050,https://doi.org/10.1021/es8007722, 2008

Kjær, H. A., Vallelonga, P., Svensson, A., Elleskov L. Kristensen, M., Tibuleac, C., Winstrup, M., and Kipfstuhl, S.: An Optical Dye Method for Continuous Determination of Acidity in Ice Cores, Environmental Science & Technology, 50, 10 485–10 493,https://doi.org/10.1021/acs.est.6b00026, pMID: 27580680, 2016.

Author comments:

We thank the reviewer for taking the time review the manuscript and provide thoughtful and constructive feedback. Reviewer comments and suggestions have been addressed; please see the below replies in blue italicized text.

Changes made to the revised manuscript in red italicized text.

Reply to RC2 (Anonymous reviewer):

The Harlan et al. paper is the latest in a series of publications on the new MBS ice core, one of the rare high-resolution records of the last millennial. Harlan et al. present the CFA dataset, including meltwater electrolytic conductivity, sodium (Na+), ammonium (NH4+), hydrogen peroxide (H2O2), and insoluble microparticle measurements.

Despite some language inconsistencies, the paper is well written and easy to read. Figures have been tested for several types of colorblindness and seem adequate in terms of colors used. The quality of the figures is good and the coherent use of colors in the different figures is appreciable.

However, I have a few concerns, especially about the lack of discussion about errors and data quality assessment, as well as a proper description of the interest and novelty of such a long and highly resolved record. The different major and minor comments are discussed below.

We thank the reviewer for acknowledging the value of our work, and for providing comments which will improve the manuscript.

Major comments:

The dataset presented here is unique, with fine resolution and spanning a millennium. However, I feel that a key point is missing, namely the emphasis on what could be done with these new records, as well as highlighting the importance of such longer time records. Readers and future users would need information on how valuable the dataset is and on its potential future use.

Thank you for highlighting the significance of the MBS CFA record. We have highlighted in the introduction (lines 31-34) some of the exciting work that has been published so far using the MBS records. We intentionally refrained from including further descriptive interpretation of the record, in regard to proxy interpretation and potential applications of the data for climate reconstruction, as the defined scope of the ESSD data descriptor manuscript type does not include interpretation or analysis of data presented. We do agree, however, that highlighting potential use cases would help to highlight the importance of this type of long, high-resolution climate record.

This is particularly important as the actual minimum resolution of this dataset is considered to be 3 cm, the same resolution as the discrete (complementary) dataset published along the paper of Vance et al. (2024a). This also raises the question: what is the value, and the reliability, of a dataset with a resolution of 1 mm? A topic only partly addressed by the authors.

Thank you for raising these concerns. We agree that this could be further clarified in the text. We will add text to the data resolution section which addresses the following points:

• While we present the 3 cm dataset as the "minimum resolution" dataset, our language was perhaps unintentionally misleading. While the effective smoothing of the peroxide

dataset from the 2018 campaign results in an effective resolution of 3 cm, every other species has lower resolution, including at or below 1 cm in the case of the conductivity signal. Resolution of 1 cm is a substantial improvement over what could be reasonably achieved with discrete sampling of a core of this length.

- In an effort to provide a concise and user-friendly dataset, we chose to provide all analytes on the same resolution (3 cm), rather than providing each analyte on the corresponding minimum depth resolution for that analyte (e.g. 1 cm for conductivity, 2.5 cm for NH4, 3 cm for H2O2), despite the fact that this underrepresents the resolution of the higher-resolution species like conductivity. Additionally, providing both a conservatively smoothed 3 cm dataset together with the 1 mm resolution dataset allows users to choose the best resolution for their particular uses.
- While the 1 mm resolution dataset is below the "actual" resolution of the dataset when accounting for data smoothing, this high-resolution dataset can be helpful in identifying extreme events in the dataset. Because the 3 cm averaged resolution dataset may smooth extreme events by reducing the amplitude and producing an artificially elevated baseline signal in the vicinity of extremes, it can be useful to provide the higher resolution dataset as a point of reference.

Text has been added to the "Dataset description" section to clarify the true resolution of the record and usefulness of the data at this resolution (l.356-359, 361-363)

On line 31, it is confusing to read a mention of ice cores in the plural when the paragraph begins with the presentation of the new Mount Brown South ice core in the singular (line 29). I think it would be interesting to first present the site and the multiple cores (currently section 1.2) and then introduce Continuous Flow Analysis (currently section 1.1). This would also provide a more logical sequence for the rest of the content. In addition, the sub-section presenting these different cores could be expanded, typically by adding information on the length and position of Alpha, Bravo and Charlie cores in relation to the main core. Consideration should also be given to adding a paragraph (or a dedicated sub-section) on what has already been done on these different cores, and possibly summarizing the main findings of Crockart et al. (2021), Jackson et al. (2023) and Vance et al. (2024a). This would also provide more clarity on the addition of this paper compared to the other publications, particularly compared to the Vance et al. paper (2024a) which already mentions the CFA data (even if it's not clear whether Vance et al. use it or not). Finally, section 4.2 on MBS chronology could be added to this part of the text instead of being presented in the data processing section (while it has not been processed in this paper).

Many good points are raised in this comment, which we will address individually point-by-point below:

• It is confusing to read a mention of ice cores in the plural when the paragraph begins with the presentation of the new Mount Brown South ice core in the singular (line 29).

We agree that we worded this in our initial manuscript in a confusing way. We will clarify in the text when we are referring to Mount Brown South (the ice core site), the Mount Brown South ice core array (ice cores plural), and the Mount Brown South ice core (the MBS-Main core specifically).

Edits have been made to clarify as suggested above.

• It would be interesting to first present the site and the multiple cores (currently section 1.2) and then introduce Continuous Flow Analysis (currently section 1.1)... In addition, the sub-section presenting these different cores could be expanded, typically by adding information on the length and position of Alpha, Brayo and Charlie cores in relation to the main core.

We will revisit these sections and introduce the ice core site (currently section 1.2) before introducing continuous flow analysis. We will also briefly introduce the Alpha, Bravo, and Charlie shallow cores, referring the reader to the MBS2023 chronology paper (Vance et al., 2024a) for further information, as we do not present any data from these cores in this manuscript.

The sections have been re-arranged, so now the manuscript reads: 1.1 Mount Brown South; 1.1.1 Ice Core Site; 1.1.2 MBS Chronology; 1.1.3 Sample description; 1.2 Continuous flow analysis...

Additional text has been added in section 1.1.1 on the four ice cores (l. 44-46).

• Consideration should also be given to adding a paragraph (or a dedicated sub-section) on what has already been done on these different cores

In lines 31-34 of the introduction, we briefly introduce some of the other works based on the MBS ice cores. As this manuscript is a data descriptor, and discussion of interpretation of other studies performed on the MBS ice cores falls outside the scope of a description of the CFA impurity record. Unless indicated otherwise by the editorial team, we would prefer to refrain from further discussions of other studies in this work.

• ...particularly compared to the Vance et al. paper (2024a) which already mentions the CFA data (even if it's not clear whether Vance et al. use it or not).

The MBS2023 chronology presented by Vance et al. (2024a) was developed prior to and independently of the production of the CFA impurity record presented here, and relied on stable water isotopes and discrete ion chemistry (as stated in l.168-169). We will clarify in these lines that MBS2023 did not use the CFA impurity record, and that this dataset is analytically independent from the data presented in Vance et al. (2024a) and the discrete ion chemistry dataset (Vance et al., 2024b).

Text has been added to the section MBS Chronology including clarification on what datasets were and were not used in its development (lines 67-69)

• Finally, section 4.2 on MBS chronology could be added to this part of the text instead of being presented in the data processing section (while it has not been processed in this paper).

We included section 4.2 in its current place in the text as we believe that the chronology information is most relevant in regards to the usage of the dataset (as we provide a decadally averaged dataset using this chronology), however understand that this could be confusing as the chronology was not produced as part of this manuscript/dataset. We will move the description of the MBS2023 chronology into the introduction, to follow our introduction of the MBS ice core site (what is currently section 1.2).

The section on the MBS chronology has been moved to section 1.1.2 (page 3).

Are there any traces of melt layers and wind crusts in the cores? Have their (potential) influences been considered in the various recordings? Even if it has been said that one of the criteria for selecting a site is a minimum of snowmelt in summer, it seems essential to document their occurrence and explain the potential influence of these melt layers and wind crusts on the recordings, especially for the 1 mm resolution dataset.

In the processing of the MBS ice core(s), we have not observed melt layers and in fact have not yet documented any melt layers across the full 295 meter Main core. Certainly, in the upper 20-25 meters of the ice core, where one would logically expect a potential increase in melt due to a warming climate, we have not recorded any observations of melt, even during summer periods. The annual mean temperature of the MBS site is -27.9 degrees C, and mean summer (DJF) air temperatures are -18.4 - cold enough to preclude melt (Vance et al., 2024a).

Nonetheless, we have observed numerous thin (~Imm thick) ice layers in the core which have been described as "bubble free layers." These features are described in Section 2.6 of Vance et al. (2024a) and are common in Antarctic ice cores (including Law Dome and WAIS among others), and while they have been poorly studied in the past, are an active area of research in the MBS cores. These features have been investigated in the Law Dome ice core in the work of Zhang et al. (2023) and are distinct from melt features. These features are also distinct from "wind crusts," but rather appear to be associated with regional scale atmospheric circulation, such as mid-latitude blocking and meridional moisture transport. Work is ongoing to investigate the chemistry and isotope signatures of these bubble free layers, and their atmospheric drivers. For the purposes of this study, the sub-millimeter scale of these features would be overcome by the internal smoothing of the CFA system, so we do not discuss them in the scope of the CFA dataset.

My major concern is the absence of any discussion of the accuracy and precision of the measurements, which is an essential point in a data paper.

Sub-section 6.3 only presents the limit of detection (LOD), i.e. the smallest concentration that can be measured by the instrument, but not how precise and accurate these measurements are. The relative standard deviation (RSD) - the standard deviation of concentrations of the standards divided by their known levels - of the lowest level standard can be used as a measure of precision, as in Griemann et al. (2022). With regard to accuracy, intermediate standards could be considered as samples (i.e. not used for calibration) and used to define the accuracy of measurements by evaluating the difference between their known concentration and the concentration measured during the run.

We disagree that accuracy and precision are not discussed, perhaps not using this exact wording, but throughout the text (i.e. in sections 5 and 6) we carefully list uncertainties and errors on the data that influence the final accuracy and precision. For example, in Section 4.1 on the depth scale, we discuss the uncertainties on depth scale and provide numbers on these and in section 6 we specifically discuss the analytical precision and data quality. However, in addition to this, we will add the relative standard deviations of the standards used (following Griemann et al. (2022), as suggested) alongside the LOD of the analytes in Table 2, as well as text describing this in Section 6.2.

Standard deviation calculations have been included in what is now Table 2, and descriptive text is included in lines 311-313.

1.267: Have you compared the 3 cm resolution Na+ dataset with Vance et al.'s (2024a) discrete dataset? This could be used as (partial) data quality assessment.

We agree that a comparison to the published discrete dataset would provide an interesting interlaboratory comparison, however we point out that this might be misleading if presented purely as a data quality assessment tool. The discrete measurements were analyzed using ion chromatography, and there is a similar (if not higher) likelihood of e.g. laboratory contamination for these measurements as for the CFA measurements.

We ultimately chose not to present a comparison to the Vance et al. (2024a) discrete dataset, as the defined scope of data description manuscripts published in ESSD states that "any comparison to other methods is beyond the scope of regular [data descriptor] articles."

Similarly, no error is mentioned for the third dataset presenting a decadal scale record. A global error calculation - including measurement and dating errors - should be associated with the decadal scale record.

We are unsure what the reviewer means by a "global error calculation" here. However, the errors associated with the measurements are described in the text of the manuscript, which is linked by DOI to the dataset as available from the Australian Antarctic Data Centre. Therefore, users of the decadal scale data set will have easy and open access to the descriptions in this text when accessing and using the dataset. Additionally, further discussion of layer counting error (as well as a comparison to the WAIS and Law Dome ice cores) is thoroughly detailed in the manuscript accompanying the MBS2023 chronology (Vance et al., 2024a), which is referenced in the manuscript text.

Section 4.4 on signal delay time is not detailed enough. Are the numbers and errors the result of statistical analysis? How many estimates have led to these values? How regularly were the bulk and individual delay times measured? And, in practice, how is the "total" delay time applied to the different measurements?

We thank the reviewer for raising the matter of delay time estimation. We will include in the text more detail on the calculation of the bulk delay times based on the individual sample runs, and how many/often standard runs were used to make these calculations.

Additional text has been added in the Signal Delay Time section, including clarification on the bulk delay time (lines 246-247), and a detail of the delay time for each analyte (lines 258-261 and a new table (now Table 1)).

I don't see how section 6.3 (1.256-261) can be used to verify data quality and depth scale accuracy. Firstly, it should be specified what data are involved here (conductivity) and the comparison between the conductivity measured by CFA and the discrete measurements of nssSO4 by Vance et al (2024a) should be clearly mentioned. Secondly, approximating 90 cm as equivalent to 3 years is not correct: it is mentioned in the text that accumulation is highly variable on an interannual scale. Moreover, even if the accumulation were more or less constant, we assume that the authors are using a sliding average of 90 cm on the raw data (observed depth), but density changes with depth, so 90 cm at the surface does not represent the same number of years as at a depth of 200 m when the snow has been compacted into ice. Thirdly, I disagree with the statement "we are able to identify many of the volcanoes reported in Vance et al. (2024a)". Looking at Table A2 in the Appendix, only 16 of the 32 volcanoes identified in Vance et al. (2024a) are also present in the conductivity record, i.e. 50%. This deserves an attempt at an explanation

(for example, it is possible that the relative proximity of the coast induces a greater presence of impurities resulting in a higher background noise in the conductivity measurements).

Based on these comments, we understand that this section of the text requires some clarifications. We do state in the text of section 6.3 that we are using the CFA conductivity measurements (presented in this manuscript), and comparing to volcanoes identified in Vance et al. (2024a), wherein the methods of volcanic identification are described. We will respond to the individual comments about the content of this section point by point below:

• I don't see how section 6.3 (1.256-261) can be used to verify data quality and depth scale accuracy.

Our intention in this section is to demonstrate the ability of the CFA record described here to correspond with signals identified in the discrete dataset. We consider that a matching eruption signal to within one year depth uncertainty is a basic validation of the general accuracy of the depth scale used to prepare this dataset. We will rephrase the opening of section 6.3 to better describe our intentions with this matching exercise.

Text has been added to section 5.3 Conductivity Peak Matching as described above (lines 315-316).

• Firstly, it should be specified what data are involved here (conductivity) and the comparison between the conductivity measured by CFA and the discrete measurements of nssSO4 by Vance et al (2024a) should be clearly mentioned.

It is stated in line 256 that we use conductivity peaks above 3 σ in this matching exercise, compared to the data provided in Vance et al. (2024a). We will add text to this section to indicate that the Vance et al., (2024a) dataset uses the non-sea salt sulfate signal to identify volcanic eruption signals.

Text has been added as described above in line 319.

• Secondly, approximating 90 cm as equivalent to 3 years is not correct: it is mentioned in the text that accumulation is highly variable on an interannual scale. Moreover, even if the accumulation were more or less constant, we assume that the authors are using a sliding average of 90 cm on the raw data (observed depth), but density changes with depth, so 90 cm at the surface does not represent the same number of years as at a depth of 200 m when the snow has been compacted into ice

We understand that 90 cm does not correspond to exactly 3 years throughout the full core, however, as we are comparing volcanic signal depths identified in the CFA conductivity to the depths of corresponding volcanic signals identified in Vance et al. (2024a), we chose to use a sliding window of fixed depth. We state in the section that this is an "approximation" of 3 years, as this is true as an average approximation across the core. As we have clearly described the accumulation variability characteristic of the site, we consider that describing this as an "approximation" is not inaccurate. We will update the text to clarify that this is indeed only an approximation and does not represent exactly three years throughout the length of the record, due to accumulation variability and density changes downcore.

Text has been added to clarify 90 cm as an approximation and why it was chosen (lines 317-318).

• Thirdly, I disagree with the statement "we are able to identify many of the volcanoes reported in Vance et al. (2024a)". Looking at Table A2 in the Appendix, only 16 of the 32 volcanoes identified in Vance et al. (2024a) are also present in the conductivity record, i.e. 50%.

We will rephrase the text in line 257-258 to the following: "Using this method, we are able to identify 16 of the 32 volcanic events reported in Vance et al. (2024a) to within one year age-at-depth uncertainty."

Proposed change has been made in revised manuscript.

• This deserves an attempt at an explanation (for example, it is possible that the relative proximity of the coast induces a greater presence of impurities resulting in a higher background noise in the conductivity measurements).

The reviewer is correct here, in that as we are comparing bulk conductivity in the CFA record with the discrete non-sea salt sulfate record, there will be inherent differences in the two datasets. However, we have intentionally avoided substantial interpretation of the record here, as ESSD specifies that significant data interpretation is beyond the scope of a data descriptor manuscript. However we will add the following statement to the text:

"We consider the ability of the CFA conductivity signal to identify half of the volcanic events found in the non-sea salt sulfate signal by Vance et al. (2024a) across the MBS record to be an external validation of the CFA conductivity record described here. We attribute existence of peaks that are not identified both datasets to the different datasets used (comparing conductivity to non-sea salt sulfate), as it is likely that some peaks in the conductivity signal are related to sources of other soluble ions, in addition to volcanic sulfate."

Text has been added to the manuscript as proposed above in lines 324-330.

Minor comments:

Some inconsistencies in the text:

Two periods of CFA measurements are mentioned in the text but using different terms (CFA sampling/measurement/melting campaign) (1.54, 1.218-219, 1.238). The same wording should be used to facilitate understanding.

We will update the text to ensure consistent wording throughout.

Proposed change has been made in revised manuscript.

The depths given for dry-drilled and wet-drilled sections are not the same throughout the text: for example, in 1.95-96, dry-drilled and wet-drilled sections are respectively at \sim 4-94 m and \sim 95-295 m vs. 5-95 m and 96-295 m in 1.218-219.

We will update the text to ensure that the relevant depth ranges are described accurately and consistently throughout the manuscript.

Proposed change has been made in revised manuscript.

There is a problem with the table numbering. The first Table mentioned in the text is actually Table 2 (line 211). The numbering of the figures and the order in which they are presented should be changed in the text accordingly.

We thank the reviewer for pointing out this error in table numbering. We ensure that the tables are presented in the correct order in the revised manuscript.

Table order has been changed to match the order in which the tables are introduced in the text.

1.2: In the abstract, the authors mention a mean annual accumulation estimated at 20-30 cm ice equivalent. However, 20 cm is never mentioned in the main text. The abstract should only contain information that is present in the main text.

We will update the abstract to reflect only the information in the manuscript.

Proposed change has been made in the revised manuscript.

Figure 1 (near 1.61): some values of lat-lon would be welcome.

We will update Figure 1 to include lat/lon values.

Lat/lon values have been added to the figure.

Legend of Figure 2 (near 1.80): "Shaded areas indicate cuts made with a bandsaw." Do you mean dotted lines?

We thank the reviewer for pointing this out. There is an error in the figure caption for Figure 2. It should state "dotted lines indicate cuts made with a bandsaw. Shaded area (hatched line) indicates surfaces planed for intermediate layer core scanning." We will update the caption to correct this.

The proposed change has been made in the revised manuscript.

1.90: A few more details on the scraping of horizontal ends could already be given here: at the very least, mention how much thickness is removed and insist that this is taken into account in the depth logs, especially as one of the datasets is published at millimeter scale.

We will add text at line 91 stating the following: "1-2 mm of ice was removed in this cleaning process. All sample pieces were measured before and after cleaning, and any ice removed in cleaning is accounted for in the depth record."

The proposed text has been added in the revised manuscript (lines 83-85).

1.95: The authors should mention why the dry-drilled section only begins at a depth of 4 meters and how the chronology of these first 4 meters is carried out.

As is common with intermediate/deep ice cores, the drilling took place from a trench dug into the firn at the ice core site. This accounts for the 4 meters missing from the top of the Main core. These 4 m were matched with the overlapping shallow cores drilled nearby during the same season. This is described in the manuscript by Vance et al. (2024a), and as we do not present the

data from the shallow cores or the chronology, we refer readers to Vance et al. (2024a) for this information.

1.114: It would be interesting for the readers to mention which type of analysis will be performed in the future.

At time of submission, it is not known exactly which analyses will be performed in the future. As such, we consider this to be beyond the scope of this data descriptor manuscript.

1.137: What are the resolution and accuracy of this cable-driven rotary encoder (in comparison to the previous system)?

The Waycon SX-80 has a sensitivity of $\gamma = 25$ counts mm-1, and linearity of +/- 0.15%. We will add text that describes the specifications of the instrument at line 137-138.

The proposed change has been made in the revised manuscript (lines 156-157)..

l.145: The last sentence of the paragraph raises a question: why would we need more details about the gas extraction system if it was not used for data collection? The answer is only 3 pages later. I suggest adding a few words alluding to the effect of gas extraction on the CFA data presented here.

Thank you for the suggestion. For brevity and to avoid unnecessary repetition, we will amend the last sentence of the paragraph to state "Further detail on the gas extraction system and its impact on measurement quality follows in section 6.1 below."

The proposed change has been made in the revised manuscript.

1.159: What is the impact of inaccuracies of one or two millimeters on the 1 mm dataset? This should be estimated and mentioned in the text.

The impact of inaccuracies on the scale of 1 - 2 mm are described in section 4.1 describing the depth scale. Such inaccuracies would be well below the annual resolution of the record and are unlikely to be of climatic interest to users of this dataset.

l.165: It is mentioned that the procedure for correcting differences in measurements of the same stick is presented in Vance et al. (2024a). However, Vance et al. (2024a) state that "The scaling and shift factors will be described in detail as the CFA trace chemistry and water isotope datasets are developed and published". So it seems that information is missing here.

We apologise for this omission. This was a two-step process: first, the depth scale for the entire Main core needed to be developed taking into account small differences in field to lab core lengths, and then also small differences in the IC (discrete chemistry) stick lengths. This is described in detail in Vance et al. (2024a). However, as the reviewer states, the shift and scaling factors (and CFA datasets) were still under development at the time of publication of Vance et al. (2024a). These discrepancies were accounted for in the assignment of the top depths for each meter-long core section. Further description of the depth scale procedures can be found in Gkinis et al. (2024). We will update the text to more clearly describe the depth adjustment process.

Text has been added to the manuscript (lines 212-218) to more clearly describe this process.

1.184: For readers unfamiliar with CFA measurements, it might be interesting to explain the principle of calibration with standards run at the beginning and end of each measurement. Is it a single calibration with some standards run at the beginning and others at the end? Or two distinct calibrations to account for e.g. measurement drifts?

The standards run procedure is relatively standardized across most CFA systems. In line 188, we refer to Kaufmann et al. (2008), wherein there is a very clear and concise description of the standard calibration procedures, which we use also here. As this is a data descriptor manuscript, and not a methods paper, we will update the text to more specifically refer the reader to the work of Kaufmann et al. (2008).

The proposed change has been made in the revised manuscript (line 231).

1.189: Shouldn't the MATLAB script mentioned be made available in a code availability section, as required by the ESSD guidelines?

The MATLAB scripts used here only perform simple calculations in an automated manner. All computations performed in the MATLAB scripts used in data processing are described in the text of the manuscript, and as such, we do not consider the scripts themselves to provide significant additional information to the reader. Additionally, the majority of similar ESSD manuscripts (e.g. Erhardt et al. (2023)) do not include scripts used for simple data processing/calibrations.

MATLAB calibration script will be included in manuscript supplement.

1.205-206: Attention should be paid to the significant figures used here (either 79 ± 4 seconds or $79.x \pm 3.6$ seconds).

We thank the reviewer for pointing this out. We will update the text to ensure consistency of significant digits throughout.

The text has been updated for consistency as described above.

1.254: Is Figure 4 needed? It is not really discussed in the text and is quite redundant with Table 2.

We find Figure 4 to be a helpful means of visualizing the range of variability of the dataset, however we will consider moving it to the supplementary materials if the manuscript length is a concern.

1.279: When mentioning "baseline values", do you mean "true" observed baseline or the limit of detection? It seems more accurate to define the LOD as a threshold.

The baseline values referred to here are the measured MilliQ (Merck RiOsTM16 MilliQ) levels. We will update the text in line 279 to clarify this.

The proposed change has been made in the revised manuscript (lines 351-352).

Figure 5:

1) The last data point of each complete series reaches 0. If this is an artifact of the plotting (which it probably is), the last point of each series should be removed.

The reviewer is correct that this is a plotting artifact. We will correct this in the revised figure.

Figures have been updated.

2) It looks like there are several points reaching 0 in the H2O2, Na+ and NH4+ series. If this is the case, these points are probably below the LOD/baseline (especially for H2O2 and Na+) and should be removed according to text line 279. It may be interesting to try to plot the LOD for these series (even though they are low for H2O2 and very low for NH4+).

As described in the reply to the comment on Line 279, MilliQ the baseline value used was the threshold for data removal (which will be clarified in the revised text). We will add the LOD to the plot in Figure 5 to provide a visual representation of the information provided in Table 2.

Dashed lines have been added to the plot in figure 5 showing the LOD.

1.286: Is there a reference to confirm that the layer thinning is negligible at this ice core site? This is surprising, given that layer thinning already has a significant effect at 80 m depth in records such as that from Philippe et al. (2016). I also recommend adding the cause of this "layer thinning" (due to strain rates) to the text, to leave no doubt for the reader.

Layer thinning is expected to be small at this site, with a bedrock depth of approximately 2000 metres, as discussed in Vance et al., 2016. However, the reviewer is correct that there will be some layer thinning due to strain across the core, and we will note this in the text. Layer thinning does not affect the use or interpretation of this dataset (which is already on an established chronology), but is of course taken into account when developing accumulation records (regardless of how small layer thinning is expected to be).

The proposed change has been made in the revised manuscript (line 364).

Technical corrections

Pay attention to sentence syntax (same word used several times in the same sentence):

1.2: the second word 'accumulation' can be deleted.

1.184: twice the word 'run' in the same sentence.

1.223-224: the first part of the second sentence (this gives a smoothing effect) repeats the first sentence (the dynamics lead to smoothing).

1.226: 'calculated' used twice in the same sentence.

1.227: similar as previous comment with 'using' and 'use'.

1.272: similar as previous comment with 'applying' and 'applies'.

We thank the reviewer for pointing these out. We will revise the text to avoid unnecessary repetition.

The proposed changes have been made in the revised manuscript.

Some inconsistencies in the writing:

1.99: lowercase after the ':' (as in 1.7 for example).

There should always be a space between the number and the units (see ESSD guidelines): 1.123, 1.163, legend of Table 1, 1.227, legends of Figures 4 and 5 (1 μ m)

(e.g. 1.152) The word 'meltrate' is sometimes written 'melt-rate'.

1.178-179: standardize the expression "a # step calibration" or "a # step calibrations".

1.218-219: interval values (in this case, depth values given in brackets) must either be joined to the dash or separated by a space, but must be consistent throughout the text (including in Table 1 or in other intervals like in 1.95-96, 1.139-140, legend of Table 1, 1.227, ...).

1.225: CFA system (with a lower-case s, for consistency).

We thank the reviewer for identifying these typographical errors and inconsistencies. We will update each instance to ensure the text is correct and consistent with ESSD guidelines.

The proposed changes have been made in the revised manuscript.

Some bibliography citations need to be revised:

General question: which order do you use to cite multiple references in text (for example, in 1.112-113)? 1.100: should be "(Bigler et al., 2011)".

1.122: should be "in Dallmayr et al. (2016)."

We will cross check the references to ensure that they are presented correctly and consistently throughout the text.

Purely technical corrections:

1.18: delete the comma before (Legrand and Mayewski, 1997).

We will correct this.

1.122: a point is missing after the citation.

We will correct this.

1.148: "The position derived *from* melt-rate data".

This is correct as written, as we refer here to the melt-rate data which was derived from the position of the core at each time step (we will revise this as "position-derived melt-rate" for clarity).

1.199: "(15 seconds for both *CFA setup* systems)".

We will revise the text to read "(15 seconds for both the 2018 and 2019 CFA setups)"

1.219: meltrate (instead of metlrate).

We will correct this.

1.220: the second parenthesis) is missing at the end of the sentence.

We will correct this.

Table 1: min-1 should be in superscript.

We will correct this.

1.229: min-1 should be in superscript.

We will correct this.

1.254: a point is missing at the end of the sentence.

We will correct this.

Legends Figures 4 and 5: perhaps the expression should be "particles > 1 μm per ml".

We will update the figures to use this phrasing.

1.272: I suggest adding a 'by' before 'applying'.

We will correct this.

Table A2: a hyphen is missing at 213.58 m.

We will correct this.

The above technical corrections have been addressed in changes to the manuscript as described.

References:

Grieman MM, Hoffmann HM, Humby JD, et al. Continuous flow analysis methods for sodium, magnesium and calcium detection in the Skytrain ice core. Journal of Glaciology. 2022;68(267):90-100. doi:10.1017/jog.2021.75

Philippe, M., Tison, J.-L., Fjøsne, K., Hubbard, B., Kjær, H. A., Lenaerts, J.T.M., Drews, R., Sheldon, S.G., DeBondt, K., Claeys, P., and Pattyn, F.: Ice core evidence for a 20th century increase in surface mass balance in coastal Dronning Maud Land, East Antarctica, The Cryosphere, 10, 2501–2516, https://doi.org/10.5194/tc-10-2501-2016, 2016.

References:

- Erhardt, T., Jensen, C. M., Adolphi, F., Kjær, H. A., Dallmayr, R., Twarloh, B., Behrens, M., Hirabayashi, M., Fukuda, K., Ogata, J., Burgay, F., Scoto, F., Crotti, I., Spagnesi, A., Maffezzoli, N., Segato, D., Paleari, C., Mekhaldi, F., Muscheler, R., Darfeuil, S., and Fischer, H.: High resolution aerosol data from the top 3.8 ka of the EGRIP ice core, Earth System Science Data Discussions, 2023, 1–21, https://doi.org/10.5194/essd-2023-176, 2023.
- Gkinis, V., Jackson, S., Abram, N.J. et al. An East Antarctic, sub-annual resolution water isotope record from the Mount Brown South Ice core. Sci Data 11, 986 (2024). https://doi.org/10.1038/s41597-024-03751-w
- Grieman M. M., Hoffmann H. M., Humby J. D., et al. Continuous flow analysis methods for sodium, magnesium and calcium detection in the Skytrain ice core. Journal of Glaciology, 68(267):90-100. doi:10.1017/jog.2021.75, 2022.
- Vance, T. R., Abram, N. J., Criscitiello, A. S., Crockart, C. K., DeCampo, A., Favier, V., Gkinis, V., Harlan, M., Jackson, S. L., Kjær, H. A., Long, C. A., Nation, M. K., Plummer, C. T., Segato, D., Spolaor, A., and Vallelonga, P. T.: An annually resolved chronology for the Mount Brown South ice cores, East Antarctica, Climate of the Past, 20, 969–990, https://doi.org/10.5194/cp-20-969-2024, 2024a.
- Vance, T. R., Abram, N. J., Gkinis, V., Harlan, M., Jackson, S., Plummer, C., Segato, D., Spolaor, A., Vallelonga, P., Nation, M. K., Long, C., and Kjær, H. A.: MBS2023 The Mount Brown South ice core chronologies and chemistry data, Ver. 1, Australian Antarctic Data Centre, https://doi.org/doi:10.26179/352b-6298, accessed: 2024-09-07, 2024b.
- Zhang, L., Vance, T. R., Fraser, A. D., Jong, L. M., Thompson, S. S., Criscitiello, A. S., and Abram, N. J.: Identifying atmospheric processes favouring the formation of bubble-free layers in the Law Dome ice core, East Antarctica, The Cryosphere, 17, 5155–5173, https://doi.org/10.5194/tc-17-5155-2023, 2023.

High resolution continuous flow analysis impurity data from the Mount Brown South ice core, East Antarctica

Margaret Harlan^{1,2,3}, Helle Astrid Kjær², Aylin de Campo^{2,4}, Anders Svensson², Thomas Blunier², Vasileios Gkinis², Sarah Jackson^{5,6}, Christopher Plummer^{7,1}, and Tessa Vance¹

Correspondence: Margaret Harlan (margaret.harlan@utas.edu.au)

Abstract. The Mount Brown South ice core (MBS 69.111 °S 86.312 °E) is a new, high resolution ice core drilled in coastal East Antarctica. With mean annual accumulation estimated to be $\frac{20-30}{30}$ cm ice equivalent accumulation throughout the length of the core ($\frac{295-290}{30}$ m), MBS represents a high resolution archive of ice core data spanning 1137 years ($\frac{873-2008}{30}$ SCE), from an area previously underrepresented by high resolution ice core data.

Here, we present a high-resolution dataset of chemistry and impurities obtained via continuous flow analysis (CFA). The dataset consists of meltwater electrolytic conductivity, sodium (Na^+), ammonium (NH_4^+), hydrogen peroxide (H_2O_2), and insoluble microparticle measurements. The data are presented in three datasets: as a 1 mm depth resolution record, 3 cm averaged record, and decadal average record. The 1 mm record represents an oversampling of the true resolution, as due to smoothing effects the actual resolution is closer to 3 cm for some species. Therefore, the 3 cm resolution dataset is considered to be the minimum true resolution given the system setup. We also describe the current Copenhagen CFA system, and provide a detailed assessment of data quality, precision, and functional resolution.

The 1 mm averaged, 3 cm averaged, and MBS2023 decadal averaged datasets are available at the Australian Antarctic Data Center: http://dx.doi.org/doi:10.26179/9tke-0s16 (Harlan et al., 2024).

1 Introduction

5

Ice cores represent some of the best proxies archives available for reconstructing past atmospheric composition, in terms of atmospheric gases as well as atmospheric aerosols. While atmospheric gases are contained and preserved in air bubbles in the ice, aerosols can be preserved as soluble and/or insoluble compounds deposited by dry deposition onto the snow surface or with the snow as wet deposition, and incorporated into the ice matrix as the snow is compressed into ice, (Legrand and Mayewski,

¹Australian Antarctic Program Partnership, Institute for Marine and Antarctic Studies, University of Tasmania, nipaluna/Hobart, Tasmania, Australia.

²Physics of Ice, Climate and Earth, Niels Bohr Institute, University of Copenhagen, Copenhagen, Denmark,

³Institute for Marine and Antarctic Studies, University of Tasmania, Battery Point 7004, Australia

⁴Victoria University of Wellington, Antarctic Research Centre, Wellington, New Zealand

⁵Climate and Environmental Physics, Physics Institute, University of Bern, Sidlerstrasse 5, Bern, Switzerland

⁶Oeschger Centre for Climate Change Research, University of Bern, Hochschulstrasse 4, Bern, Switzerland

⁷Australian Antarctic Division, Department of Climate Change, Energy, the Environment and Water, Kingston, Tasmania, Australia

1997). The chemical compounds from such aerosols can be measured in the ice itself, either by the chemical composition of the ice (ionic species), or by measuring the insoluble particulate material in the ice.

Many of the aerosol impurities contained in ice cores reflect seasonal variability of aerosol species. However, reconstructing seasonal cycles requires sampling resolution high enough for the seasonal signal to be resolved. This can present measurement challenges, as discrete measurements of trace chemistry of ice samples can require intensive manual decontamination of sampling, which is time consuming and can be difficult to achieve under cold laboratory conditions. Decontamination is especially labor intensive when centimeter-scale measurements are required for ice cores that range from hundreds to thousands of meters in length. Continuous flow analysis (CFA) chemistry measurements, pioneered by Sigg et al. (1994), allows allow entire lengths of ice core to be sampled continuously in high resolution with very minimal sample decontamination required (Bigler et al., 2011; Kaufmann et al., 2008; Erhardt et al., 2022).

The new Mount Brown South ice core array (MBS), one of only two the few millennial length ice cores in coastal East Antarctica (together with the Law Dome ice core), represents an important new paleoclimate record from an under-represented region in Antarctica (Vance et al., 2016, 2024a). Data from the upper (satellite-era) sections of the four MBS ice cores has have been used to investigate an East Antarctic proxy for El Niño variability (Crockart et al., 2021), as well as to understand precipitation climatology effects on the water-isotope record for the coastal East Antarctic site (Jackson et al., 2023). The full length of the MBS main core has been dated and the chronology (MBS2023, used here) is described in Vance et al. (2024a).

Here we present the high-resolution, CFA record of chemistry and insoluble impurity measurements for the full length of the MBS Main ice core. The data set is presented alongside a description of the analytical system and methodology, as well as considerations about data quality and uncertainties in both the concentration and the depth/temporal resolution of the record.

1.1 Continuous Flow Analysis Mount Brown South

35

CFA is particularly well suited for measuring trace chemical species and impurities at high resolution (millimeter to centimeter scale) for long ice cores (Bigler et al., 2011). This allows for the production of seasonal-scale records of aerosol species spanning thousands of years at sites with sufficiently high accumulation. CFA is advantageous compared to discrete methods such as ion chromatography, as it provides the ability to analyze ice core samples at speeds of up to four centimeters per minute and with minimal time required for decontamination and sample changeover.

The CFA process involves melting a vertical section of an ice core (typically from top to bottom) by placing it on a purpose-built heated plate (melthead) connected to a melt water extraction system. The melthead is designed to prevent contamination, such that the external portion of the core section is diverted to waste and thus manual decontamination is only required along the horizontal surfaces at core breaks. The inner decontaminated melt water is debubbled and subsequently diverted through a system of measurement instrumentation using a series of peristaltic pumps. Measurements are taken continuously (data recorded each second). The detectors used are chosen for their short response time and ability to detect the low impurity concentrations observed in polar ice (Sigg et al., 1994).

The modular nature of CFA allows it to be simplified for deployment to the field for in-situ measurements (Kjær et al., 2021). It may also be expanded for additional gas (Stowasser et al., 2012; Rhodes et al., 2013) and isotope (Gkinis et al., 2011; Jones et al., 2017).

measurements in addition to chemistry and impurities (Bigler et al., 2011). The Copenhagen CFA setup used in the 2018 and 2019 MBS campaigns both build on the CFA setup described in Bigler et al. (2011) and Kjær et al. (2022). Both campaigns used the same system components, however, the entire CFA system was relocated to a new building between campaigns. The move resulted in some differences between the setups, which are detailed below.

The chemistry and impurity measurements from both campaigns include insoluble microparticles (dust > 1 μ m), electrolytic conductivity, calcium (Ca²⁺), sodium (Na⁺), ammonium (NH₄⁺), hydrogen peroxide (H₂O₂), and meltwater acidity. Additionally, sulfate (SO₄²⁻) was analysed in 2018. The acidity, sulfate, and calcium records, however, are not presented here, due to independent problems with the measurement systems for those species.

1.2 Ice core site

Map showing the location of the Mount Brown South site.

Four ice cores were drilled during the 2017-2018 austral summer field season at the coastal East Antarctic Mount Brown South site (MBS1718-Main, -Alpha, -Bravo, and -Charlie). The MBS-Main Here we present CFA data for the MBS1718-Main core only.

1.1.1 Ice core site

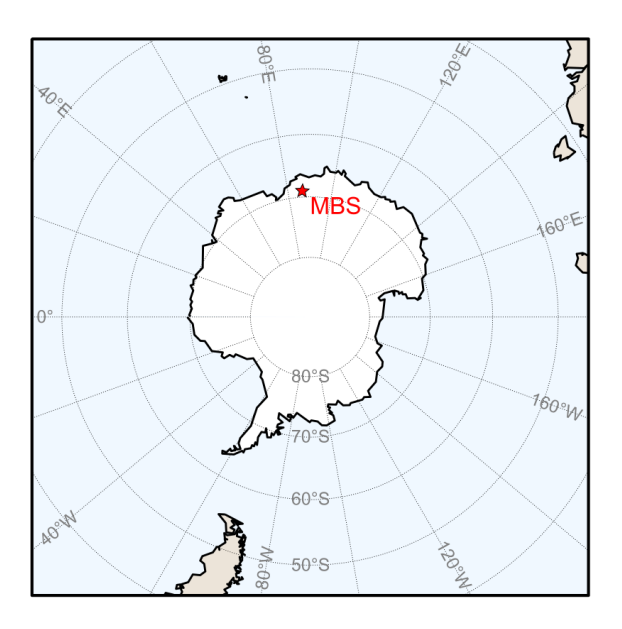


Figure 1. Map showing the location of the Mount Brown South site.

The Main core drill site lies at 69.111°S, 86.312°E, 2084 meters ASL, adjacent to the boundary between Princess Elizabeth and Wilhelm II Land, approximately 62 km south of the Mount Brown nunatak, and located 12.6 km WSW of a short surface core drilled in December 1998 (known as "MBS99," Smith et al. (2002); Foster et al. (2006)). The three MBS shallow cores (Alpha, Bravo, and Charlie), were drilled nearby (within 100 m of the main core site) to depths of 20.41, 20.225, and 25.86 m, respectively, but data from these cores are not included in this dataset.

While the four cores drilled during the 2017-2018 season are named MBS1718, for simplicity, we refer to them here as simply MBS. The MBS site was selected based on six criteria as described in Vance et al. (2016) in order to (1) preserve a millennial-scale record in the 300 meter archive; (2) undergo minimum snowmelt in summer; (3) preserve sub-annual resolution (minimum accumulation of 25 cm/yr ice equivalent); (4) experience minimal surface reworking; (5) have undergone minimal ice advection at 300 m depth; and (6) add novel information to the existing network of East Antarctic ice cores. Average accumulation at the site is found to be 30 cm ice equivalent per year over the satellite era (1978 to 2017, based on annual layer depth counting of the shallow cores) (Crockart et al., 2021) and the site is characterized by wet deposition (Crockart et al., 2021; Vance et al., 2024a). Mean annual surface air temperature at the MBS site is -29.7°C (based on the Modèle Atmosphérique Régional (MAR) regional climate model, Agosta et al. (2019)), and the site is characterized by predominantly easterly prevailing winds (Vance et al., 2024a). Drill site characteristics for MBS the MBS site are presented in Vance et al. (2024a) and detailed climatology of the site is well described by Jackson et al. (2023) and Crockart et al. (2021).

Vance et al. (2024a) presents the MBS2023 chronology, a combined depth-age scale for MBS1718-Main and MBS1718-Charlie. The 295 meters of the main core cover MBS-Main and MBS-Charlie. The main core covers 1137 years (873-2008 CE), while the three co-located surface cores (Alpha, Bravo, and Charlie) cover approximately the satellite era through to drilling year (2017-2018).

2 Sample description

1.0.1 MBS chronology

An age scale has been developed for the MBS ice cores, described thoroughly in Vance et al. (2024a). The ice core dating and layer counting was based on a combination of stable water isotopes (Gkinis et al., 2024b) and discrete chemistry measurements, primarily the ratio of sulfate to chloride, and there was found to be significant variability in annual layer thickness throughout the length of the core. The chronology was determined by two independent layer counting efforts, one relying on volcanic matching, the other primarily relying on variable chemistry species. These two efforts were followed by careful consideration and joint determination of uncertain years (Vance et al., 2024a). Development of the MBS2023 chronology did not rely on the CFA impurity record, and the CFA dataset presented here is analytically independent from the discrete dataset and chronology presented in Vance et al. (2024b). We encourage direct users of the MBS CFA dataset to use the MBS2023 chronology (Vance et al., 2024b), or any subsequent updates thereafter.

1.0.2 Sample description

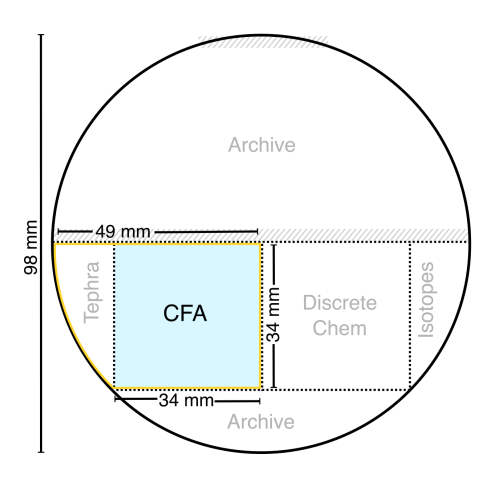


Figure 2. Schematic diagram showing the cross-section of the MBS main core, with sample sections shown. Shaded areas Dotted lines indicate cuts made with a bandsaw. Dashed lines indicate Shaded area (hatched line) indicates surfaces planed for intermediate layer core scanning. Section shipped to Copenhagen shown outlined in yellow, with CFA stick shaded in blue.

100 from a depth of 4.25 m (depth at the top of the borehole, accounting for the recessed floor of the drilling tent and drill trench) to 294.79 m depth using the Danish Hans Tausen ice core drill (9.8 cm core diameter). The ice was transported from the drill site to Hobart, where it was described (in terms of core quality, including breaks, cracks, and other damage to the core), logged, and imaged in the -18°C freezer laboratories at the Institute for Marine and Antarctic Studies. There, it was sectioned lengthwise for analyses. An interior piece with 34 x 34 mm cross section area along the entire length of core was designated for CFA chemistry (Fig. 2). See Vance et al. (2024a) for a full description of the ice processing.

The CFA section, still attached to the wedge-shaped outer edge piece designated for tephra sampling, was transported to Copenhagen, where the samples were prepared for CFA by removing said outer wedge at freezer facilities at the Physics for Ice, Climate and Earth (PICE) at the Niels Bohr Institute (NBI). To minimize potential contamination, the horizontal ends of each sample piece, including any breaks occurring within a sample, were carefully cleaned by scraping with a ceramic blade immediately prior to being placed in frames for melting on the Copenhagen CFA. Approximately 1-2 mm of ice was removed from each break in the ice in this cleaning process. All sample pieces were measured both before and after cleaning, and any ice removed in cleaning has been accounted for in the depth record.

1.1 Continuous flow analysis

CFA is particularly well suited for measuring trace chemical species and impurities at high resolution (millimeter to centimeter scale) for long ice cores (Sigg et al., 1994; Bigler et al., 2011; Erhardt et al., 2022). This allows for the production of seasonal-scale records of aerosol species spanning thousands of years at sites with sufficiently high accumulation. CFA is advantageous

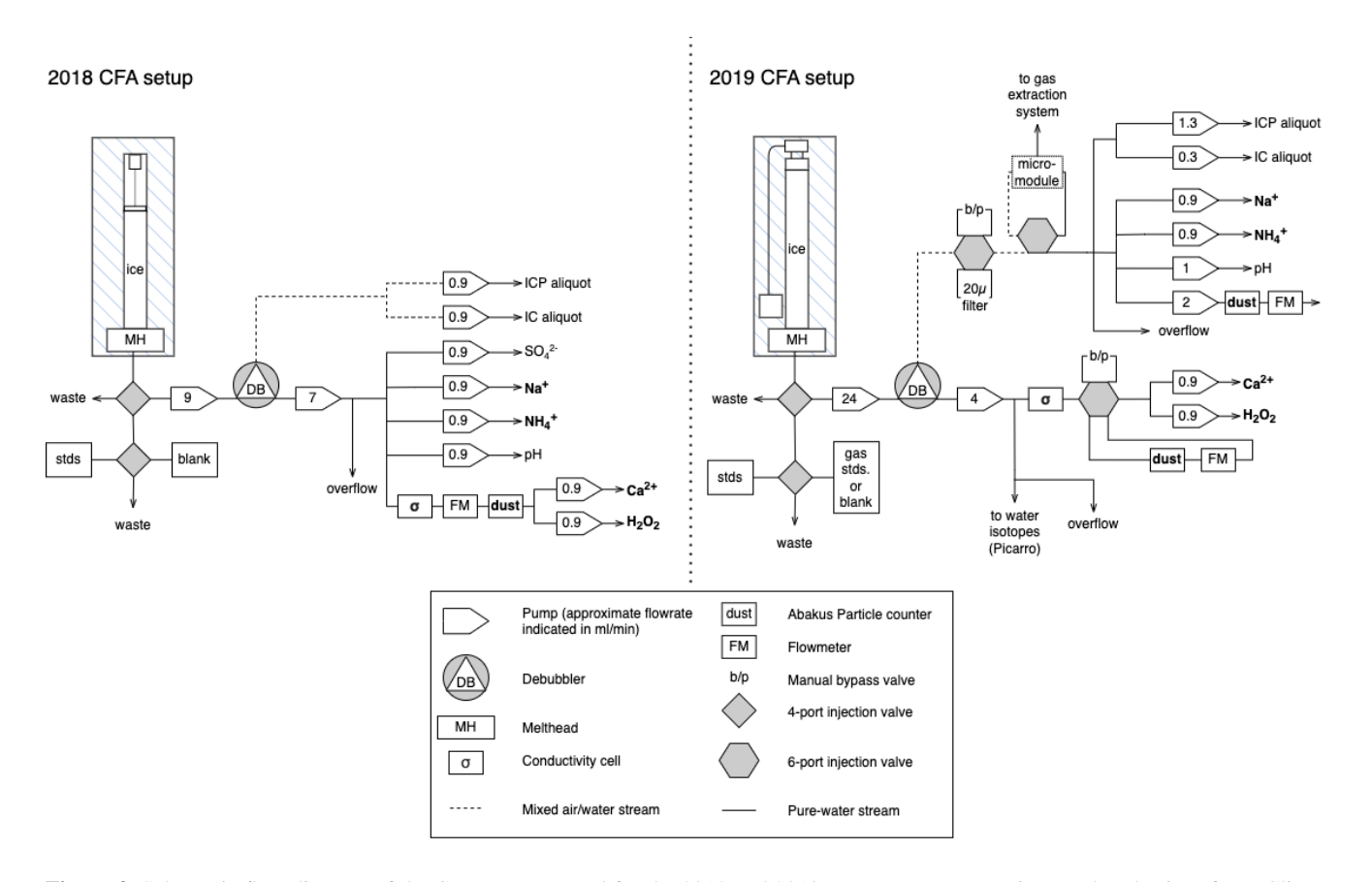


Figure 3. Schematic flow diagram of the CFA systems used for the 2018 and 2019 measurement campaigns at the Physics of Ice, Climate, and Earth in Copenhagen.

compared to discrete methods such as ion chromatography, as it provides the ability to analyze ice core samples at speeds of up to four centimeters per minute and with minimal time required for decontamination and sample changeover (Röthlisberger et al., 2000; Kau

The CFA process involves melting a vertical section of an ice core (typically from top to bottom) by placing it on a purpose-built heated plate (melthead) connected to a melt water extraction system. The melthead used in the Copenhagen CFA system is designed to prevent contamination, such that the external portion of the core section is diverted to waste and thus manual decontamination is only required along the horizontal surfaces at core breaks (Bigler et al., 2011). The inner decontaminated melt water is debubbled and subsequently diverted through a system of measurement instrumentation using a series of peristaltic pumps. Measurements are taken continuously, with data recorded each second (Kaufmann et al., 2008). The detectors used are chosen for their short response time and ability to detect the low impurity concentrations observed in polar ice (Sigg et al., 1994; Röthlisberger et al., 2000).

The modular nature of CFA allows it to be simplified for deployment to the field for in-situ measurements (Kjær et al., 2021). It may also be expanded for additional gas (Stowasser et al., 2012; Rhodes et al., 2013) and isotope (Gkinis et al., 2011; Jones et al., 2017) measurements in addition to chemistry and impurities (Bigler et al., 2011). The Copenhagen CFA setups used in the 2018 and 2019 MBS campaigns both build on the CFA setup described in Bigler et al. (2011) and Kjær et al. (2022). Both campaigns used the same system components, however, the entire CFA system was relocated to a new building between campaigns. The move resulted in some differences between the setups, which are detailed below.

The chemistry and impurity measurements from both campaigns include insoluble microparticles (dust > 1 μ m), electrolytic conductivity, calcium (Ca²⁺), sodium (Na⁺), ammonium (NH₊), hydrogen peroxide (H₂O₂), and meltwater acidity. Additionally, sulfate (SO₄²⁻) was analysed in 2018. The acidity, sulfate, and calcium records, however, are not presented here, due to independent problems with the measurement systems for those species.

2 MBS continuous flow analysis

130

135

140

145

155

The basic setup of the Copenhagen CFA system is well described in Bigler et al. (2011) and Kjær et al. (2022), and is based on previous CFA systems such as Kaufmann et al. (2008) and Röthlisberger et al. (2000). The CFA measurements took place over two sampling campaigns. The dry-drilled section (~4-94 m-5-95 m depth) of the main core, and the Charlie core (25.86 m) were analyzed in 2018. The remaining (wet-drilled) section of the main core (~95-295 m depth) was analyzed in 2019 after the CFA laboratory was relocated to another building. Flow diagrams for the two systems used for the MBS CFA measurements can be seen in Fig. 3. Details of adaptations to the system made between the two campaigns are described below.

The CFA base functionalities are very similar between the two analytical campaigns: Sticks of firn/ice are placed into polycarbonate frames for mounting above the melter system consisting of the heated melthead (Bigler et al. (2011)) (Bigler et al., 2011) and above it a short ice alignment guide (~20 cm), all held inside a freestanding freezer unit maintained at approximately -20°C. The frames and alignment guide allow for each new stick of ice to be added to the system before the previous stick is fully melted. This allows for continuous melting of multiple (typically 5-10) meters of ice during each run similar to the CFA procedure described in Erhardt et al. (2023) and Kjær et al. (2022).

As the ice is melted, meltwater from the clean interior of the sample is pumped to the analytical systems using peristaltic pumps (ISMATEC), while water from the potentially contaminated outer ice is diverted to waste. Both setups employ the use of an enclosed debubbler consisting of a flat triangular cell to remove air bubbles from the sample stream (Bigler et al., 2011). Both systems utilize a commercially available conductivity meter to measure meltwater electrolytic conductivity, as well as an Abakus laser particle counter (LDS23/25bs; Klotz GmbH, Germany) coupled with a flowmeter to determine the number of insoluble particles larger than 1 μm per ml of sample volume (Simonsen et al., 2018). Simple fluorescence or absorption spectroscopic methods are used to determine NH₄⁺, Ca²⁺, H₂O₂, Na⁺, SO₄²⁻, and meltwater acidity, using instrumentation and methods specifically designed for CFA (Kaufmann et al., 2008; Sigg et al., 1994; Röthlisberger et al., 2000; Erhardt et al., 2022; Kjær et al., 2016). Reagents and buffers for analysis were prepared weekly or bi-weekly as required with respect to their rate of deterioration. Additionally, during both campaigns, aliquots were collected in vials for later analysis

using ion chromatography (IC) and inductively coupled plasma mass spectrometry (ICP-MS), the results of which are not included in this dataset and will be released in a future publication.

2.0.1 Specifics for the 2018 CFA setup

2.1 Specifics for the 2018 CFA setup

The 2018 CFA measurements took place at the Center for Ice and Climate at the University of Copenhagen in the laboratory described also by Simonsen et al. (2019) (which at that point was located at Juliane Maries Vej Copenhagen) during October-November 2018.

An optical depth registration system (Waycon LLD-150-R5232-50H) was used for registration of the melt speed during the 2018 campaign, in a setup similar to that used in (Dallmayr et al., 2016) Dallmayr et al. (2016). While the laser distance meter allows for precise melt speed and sample length measurements (± 2mm 2 mm accuracy, and 0.5 mm resolution), it can be temperamental as vibrations from ambient activity (heavy footfalls or accidental knocking of the freezer enclosure) can disrupt measurements. Additionally, the ice is never a perfect fit to the frame and as it melts it changes from leaning on one side of the frame to the next causing some additional noise seen in the very precise laser measurement. Additionally, the space required for the laser system limits the length of the frames used in the freezer, thus limiting the sample stick length to 50 cm. For the campaign in 2018, 10 sample sticks (5 m) were melted continuously per run, book-ended by standards runs (see section 4.3 and table-Table A1).

A sulfate measurement system following the method used for NorthGRIP (Kaufmann et al., 2008; Erhardt et al., 2022) was trialed in the 2018 system, but due to a high limit of detection of the system, sulfate measurements were unsuccessful, and thus are not presented here. Discrete sulfate measurements of the full MBS record via ion chromatography can be found in Vance et al. (2024a).

2.1.1 Specifics for the 2019 CFA setup

175

180

2.2 Specifics for the 2019 CFA setup

In October-November 2019 the Physics of Ice, Climate, and Earth at the University of Copenhagen moved to a new address at Tagensvej 16. Due to the relocation the 2018 system was dismantled and rebuilt in the new location. During reassembly changes were made to the system, described herein.

A cable-driven rotary encoder (draw wire position transducer, SX80, WayCon; sensitivity: $\gamma = 25$ counts mm⁻¹, linearity: $\pm 0.15\%$) was implemented for depth registration in 2019 similar to that described in Bigler et al. (2011). This encoder setup freed up more space in the freezer unit, allowing for melting of meter long sample sticks and thus the data from the 2019 campaign has fewer sample breaks per run as 5-10 samples (5-10 m) were melted continuously per run. Further, all chemistry lines were optimized in length to minimize dispersion and thus smoothing of the final record.

As part of the 2019 rebuild, a gas extraction system (3M, Liqui-Cel MM-0.75×1 Series) coupled to the mixed air-water stream from the top of the debubbler unit was added to the CFA. While the gas extraction system was not used for data collection during the MBS melting campaign, it was sporadically implemented for testing and refinement throughout the 2019 measurements. Further detail on the gas extraction system follows and its impact on measurement quality follows in section 5.1 below.

2.3 Primary differences between 2018 and 2019 CFA setups

195

210

As described above, the two system setups used in the MBS CFA measurements are largely similar, using much of the same equipment and instrumentation. The primary differences, and their potential impact on measurements between the two setups are as follows.

- Depth registration system: The 2018 setup utilized a laser distance meter reflecting off of a weight placed on top of the ice, while the 2019 setup used a cable-driven rotary encoder attached to a weight resting on the top of the ice. Additionally, the two instruments result in different amounts of "downtime" in the system during ice stick frame changeover, with slightly more time required when changing frames with the rotary encoder system. While these factors might influence the resulting CFA depth scale, these offsets can be cross-checked with the lengths measured in the freezer during sample preparation. That these differences are minimal, and likely within the scope of the measurement error of the instrumentation.
 - Ice stick length: Due differences in depth registration instrumentation (the laser distance meter takes up substantially more vertical height than the draw-wire encoder in the limited freezer height), approximately 55 cm long ice sticks were used in 2018 and 100 cm long sticks were used in 2019. The 55 cm ice sticks introduce additional breaks in the ice which may introduce more potential contamination than with the 100 cm ice sticks. However, the 55 cm ice sticks have the advantage of allowing increased certainty of absolute depths, as the lab-measured top depths are known every 55 cm.
 - Meltrate The ice meltrate was slightly different for the two setups. The impact of the meltrate on sample smoothing and
 resolution is discussed further in section 4.1.
- Gas extraction system and stable water isotope measurement The 2019 setup introduced both a gas extraction system and an in-line cavity ring-down spectrometer (Picarro L-2140i) for stable water isotope measurements. The gas extraction system is described in more detail in section 5.1, and the stable water isotope measurements are described in Gkinis et al. (2024b). As the gas extraction system required a higher sample volume, the pumped flow rates through the system was different between the two setups (see approximate flow rates in Fig. 3). This resulted in more overflow routed to waste per minute of melting in the 2018 setup than in the 2019 setup. Notably, the target flowrate through each individual measurement instrument is similar for both systems (e.g. ∼1 ml min⁻¹ for each chemistry line and ~2 ml min⁻¹ for the conductivity and dust measurement lines; target flowrates for each analyte presented in Fig. 3).

3 Data processing

3.1 Depth scale

225

230

235

240

245

250

Precise depth information is crucial for ice core data. The position derived melt-rate position-derived meltrate data collected during CFA campaigns is used to reconstruct the total length of ice melted, to which the recorded length of ice removed during preparation must be re-introduced at the appropriate depths. To account for the time when the encoder is removed during the frame changes, for both the laser and draw-wire encoder, the position data is used to identify the times just before and after each frame change period, and the average meltrate over the previous period of uninterrupted melting is used to reconstruct a continuous melt-rate. meltrate. The down-time that occurs during frame changeover is slightly longer for the draw-wire encoder than that of the laser encoder, as the draw-wire assembly that is attached to the encoder must be fully removed from the remaining ice and subsequently replaced once the new frame has been mounted.

The information recorded during sample preparation is used (including ice removed for decontamination at sample ends and breaks and poor-quality ice not analyzed), together with the position of each break as logged during melting, to create appropriately sized gaps in the depth scale corresponding to the missing ice. The depth scale is finalized by assigning the top of each CFA data run to the recorded top depth of the corresponding bag from the agreed upon field depth measurements. Manual decontamination of the cores can introduce slight (sub-millimeter) discrepancies due to mis-reading lengths on the standard ruler used in preparation as well as slight misjudgments and biases in identification of break positions during melting. These unavoidable inaccuracies are estimated to be on the scale of one or two millimeters at most.

In rare cases, measured lengths of the same stick varied from one measurement to another (for example, when measured in Hobart prior to shipping to Copenhagen). This was found to be due to slightly slanted cuts where one core meets the next, with one measurement taken from the long side and another taken from the short side. These discrepancies were found to amount to less than 0.01 % of the length of the record (Gkinis et al., 2024b). Careful consultation of comprehensive line scan images of the core sections were was used to correct for these errors and determine an agreed upon core length across all measurements. This procedure process required the depth scale for the entire Main core to be developed, taking into account small differences in field to lab core lengths as well as any small discrepancies in the IC (discrete chemistry) stick lengths. This is described in detail in Vance et al. (2024a).

3.2 MBS Chronology

An age scale has been developed for the MBS ice cores, described thoroughly in Vance et al. (2024a). The ice core dating and layer counting was based on a combination of stable water isotopes (Gkinis et al., 2024a) and discrete chemistry measurements, primarily the ratio of sulfate to chloride, and there was found to be significant variability in annual layer thickness throughout the length of the coreAny such differences were accounted for in the development of the CFA depth scale in the precise assignment of the top depths for each meter-long core section. This top depth assignment was done to prevent any small discrepancies from propagating through the length of the core. Additional description of the depth scale procedures can be found in Gkinis et al. (2024b). The chronology was determined by two independent layer counting efforts, one relying on

volcanic matching, the other primarily relying on variable chemistry species. These two efforts were followed by careful consideration and joint determination of uncertain years (Vance et al., 2024a). We encourage direct users of the MBS CFA dataset to use the MBS2023 chronology (Vance et al., 2024b), or any subsequent updates thereafter.

3.2 Calibrations

260

265

270

275

280

285

The absorption and fluorescence spectrometric methods used for chemistry concentration measurements require calibration to convert from instrument signal voltage/light intensity to concentration. In order to properly calibrate these instruments, standard solutions with predetermined chemical concentrations are passed through the system before and after each sample run. A multi-element standard solution is used for a three step calibration of the Ca²⁺, Na⁺, and NH₄⁺ measurements (Merck Certipur®IC Multi-element Standard VII). A single component standard solution solution is used for a two step calibrations calibration of H₂O₂ (Sigma-Aldrich Hydrogen Peroxide Solution 30 wt % in H₂O). The multi-element standard solutions are prepared prior to each run, and the peroxide standards are prepared prior to each run from a first dilution prepared at the start of each measurement day. All standards are prepared using ultra-pure deionized water (Merck RiOsTM16 MilliQMilli-Q®). Standard recipes and resulting concentrations are presented in Table A1.

Calibrations are calculated from the standards, which were run at the beginning and end of each measurement run—, as described in Kaufmann et al. (2008) and Erhardt et al. (2023). This allows for monitoring of system drift and provides ample standards data for each run, in case any issues arise during a standards run. Each standard solution is passed through the system in series and the resulting signal voltage was recorded both manually and by the LabVIEW software used to operate the system. For the fluorescence method (Ca²⁺, NH₄⁺, and H₂O₂ measurements), the standard calibration is based on the linear relationship between concentration and fluorescence signal voltage. Sodium is a pseudo-absorption method, and calibration is based on a curve fit to the standard signal response (Kaufmann et al., 2008). Calibrations are computed using a semi-automated script written in MATLAB. The script isolates the signal voltage at each standard input concentration and calculates the appropriate calibration coefficients. The standards are well fitted, with the average r-square value for the calibration curves for each analyte being greater than 0.99.

3.3 Signal delay time

Due to differing distances of each of the measurement instruments from the melter, there is a time delay between when the ice passes the melter and when the measurement takes place.

The time delay between the ice on melter and when the measurement is recorded down stream is calculated in two parts. Firstly, there is the elapsed time from when the sample parcel passes the melter to when it is divided into disparate melt streams for each analytical unit. The bulk melt delay time is measured during sample melting as the elapsed time from when the first sample ice passes the melter (recorded as observed by lab operator) and the initial peak response observed in the conductivity measurements (15 seconds for both systems). Conductivity is used as it is located closest to the melter (by tubing distance/mixing volume as well as time), and thus the first signal to respond. In both systems, the approximate total time offset between the sample ice reaching the melter and the response seen in the conductivity signal was approximately 40 seconds.

Secondly, there is a delay time individual to each species measured due to the internal dynamics of each analytical melt stream. These response delay calculations are computed based on each instrument response time during the standard runruns. This additional delay time is measured as the time elapsed between when the signal increase is seen in the conductivity measurements and target species. We determined that additional delay time as time at which the derivative of the response curve of the standards reaches a maximum (approximating the midpoint of the sample response rise). Delay time varies The average delay time (from all standards runs used in calibration) is presented in Table 1.

Delay times vary for each species: 79, but are similar between the two system setups (Table 1). Other choices for delay calculations could have been to use the start of the rise or even the end of the rise, however due to smoothing can be hard to reliably identify, whereas the maximum of the derivative of the increase is easily and systematically identified. However, we recognize that this can introduce a minor offset between methods that are highly smoothed in comparison to those that have faster response times.

Table 1. Average delay time in seconds for each analyte measured as elapsed time between conductivity signal response and analyte signal response, based on the maximum of the first derivative of the signal response measured during each standards run.

	2018 (5-95 m depth)	2019 (95-295 m depth)
	Delay time (seconds)	Delay time (seconds)
	mean ± 3.6 seconds for std. dev. (n = 18)	$\frac{\text{mean} \pm \text{std. dev. } (n = 29)}{\text{mean} \pm \text{std. dev. } (n = 29)}$
Ca ²⁺ , 73	69 ± 5.9 seconds for 9	79 ± 4 20 ± 4
$NH_4^+, 48$	66 ± 5.3 seconds for 9	74 ± 9 ≈ × × × ×
H_2O_2 , and	<u>62 ± 11</u>	$68 \pm 4.0 \frac{4}{\text{seconds for 4}}$
Na ⁺ -	<u>58 ± 7</u>	48 ± 8

As the delay times can vary slightly from run to run, due to factors including tubing length, tubing wear, and fluctuations in melt speed, delay times for each species were measured and applied individually to each CFA run of 5-10 m of ice melted. Each delay time estimation was calculated based on the standards data collected either immediately prior to or following the run.

3.4 Calcium data

305

290

295

Expected concentrations of calcium at the MBS site are very low (median chemistry concentration from the discrete chemistry measurements is 0.142 ppb). Due to the nature of the system, and the limits of the ultrapure water system used to produce the standards, reagents, and baseline values for measurements produced here, this is significantly below the limit of detection we are reliably able to achieve using the Copenhagen CFA system (see Table 2). As the CFA Ca²⁺ data for MBS does not show any discernible seasonal cycles throughout the record, and the calibrated Ca²⁺ concentration values measured close to or below the LOD of our instrumentation, we consider these values too low to report.

4 Data resolution and smoothing

4.0.1 Sampling resolution

310

315

320

325

330

335

4.1 Sampling resolution

Data is registered at one second time steps, and thus the sampling resolution varies with meltrate. The meltrate of the CFA system is selected to optimize resolution, while accounting for density changes from firn to ice, however with the introduction of the gas extraction system in 2019, the meltrate was calibrated to produce optimal gas volumes for simultaneous measurement. The 2018 system setup (5 – 95 m depth) CFA setup operated with a target meltrate of 3.5 ~4.5 cm min⁻¹ throughout the upper 35 m depth, decreasing across 10 m to reach ~3 cm min⁻¹ below 45 m depth (median actual meltrate meltrate 3.45 cm min⁻¹ across the full 2018 record). The 2019 campaign (96-295~95-295 m depth) had a target meltrate of 4 cm min⁻¹ (median actual meltrate 4.08 cm min⁻¹. These). These median meltrates produce a direct sampling resolution (independent of smoothing due to response time) of 0.58 and 0.68 mm, respectively.

4.1.1 Signal dispersion smoothing

4.2 Signal dispersion smoothing

The internal dynamics of the system (mixing volumes and flow conditions within tubing) lead to smoothing due to signal dispersion, as described by Breton et al. (2012). This gives a smoothing effect, wherein a discrete parcel of sample is measured in the CFA System system as a dispersed signal spread across a short time period (on the order of a few seconds) spanning the expected signal response time for that parcel (Breton et al., 2012). This dispersion time is calculated as as an e-folding time calculated based on the 10 - 9010-90 % rise time in the signal response during the standards runs. Using run. Based on the meltrate, it is possible to use this dispersion signal time to calculate the effective smoothing length (and thus a minimum realistic resolution) for each species (Table ??). Although the meltrate used in 2019 was faster than in 2018 (4.08 and 3.45 cm min=1-1 respectively), the shorter response times (likely due to shorter tubing lengths used in the rebuilt system) resulted in a higher resolution in 2019.

It is worth noting that, as described by Breton et al. (2012), the signal peak under realized (dispersed) flow conditions occurs slightly before the expected signal response under idealized "plug flow" conditions. This effect is linked to the specific dynamics of each CFA system, and similar to Erhardt et al. (2022), we do not quantify this slight offset for the Copenhagen system, but note that it could lead to a slight systematic offset (on the order of a few millimeters) biased towards deeper shallower sample depths.

Table 2. Response time as 10%-90% rise time (t_{10-90}) Sample data range and e-folding time (τ_e) LOD for all measured species, and resultant effective smoothing length based on meltrate standard deviation (resolutionSD). Values shown of lowest-concentration standard for each of the two system setups from 2018 and 2019 (and the depths measured during each campaign) chemistry analyte.

	2018 (5-95 m depth)				2019 (95-295 m	
	Range	Median	LOD	\underbrace{SD}	Range	<u>Me</u>
	t_{10-90} (s(5th & 95th percentile)	$ au_e$	resolution (cm	(ppb)	$t_{10=90}$ (s(5th & 95th percentile)	7
Conductivity ($\mu \text{S cm}^{-1}$)	17.5 0.74 - 1.55	8.0 -1.03	1.01 _0.01	9.8-	4.4 0.57 - 1.38	0.67
$\underbrace{\operatorname{Dust}(\#\operatorname{ml}^{-1})^*}$	97.32 - 707.20	281.99	25.00		- -	
Ca ²⁺ (ppb)*	\bar{z}	-~	0.82	1.93		
NH ₄ (ppb)	41.7 0.07 - 1.03	19.0 0.32	2.39 0.03	35.3 - <u>1.37</u>	16.1 _0.09 - 0.87	2.40
H_2O_2 (ppb)	52.9 <u>6.84</u> - 69.92	24.1 - <u>26.82</u>	3.04_0.65	41.0- 3.31	18.6 -5.40 - 49.01	2.79 2
Na ⁺ (ppb)	41.6- 2.39 - 38.89	18.9 - <u>13.54</u>	2.39 <u>4.26</u>	33.3 - <u>1.82</u>	15.1 -3.01 - 36.41	2.24

^{*} Dashes indicate data not included in the published dataset.

5 Uncertainties and data quality

340

345

350

5.1 Gas extraction system interference

During the 2019 CFA melting campaign, the introduction of a new gas extraction system was trialed. This system setup comprised a gas extraction line originating from the upper outlet of the debubbler, coupled to a micro-module which extracts dry air from the sample stream for gas analysis. These system trials influenced the internal pressure balance of the chemistry system tubing. This had a significant impact on the meltwater acidity (pH) measurements (Kjær et al., 2016), which suffered from back pressure changes influencing the sensitive dye to water ratios, making the pH record unusable. The gas extraction system also impacted the insoluble microparticle data collected by the ABAKUS laser particle counter.

While the specifics of the gas extraction system are beyond the scope of this data description, there is a visible signature in the microparticle record that only occurs when the gas extraction system was on-line with the chemistry CFA. The signature can be seen as a significantly elevated baseline in the microparticle record (measured from Milli-Q@ultrapure water through the system), as well as an alteration in the amplitude of the dust signal. These changes correspond with the recorded valve switches of the gas system. Due to the nature of the system interference, we are not able to reliably correct for this interference. We therefore only present the insoluble microparticle data for the dry drilled section (5-95 m), 5-85 m depth, measured in 2018 before the gas system testing began.

Table 3. Sample data range—Response time as 10-90 % rise time (t_{10-90}) and LOD—e-folding time (τ_e) and resultant effective smoothing length based on meltrate (resolution). Values shown for each analyteof the two system setups from 2018 and 2019 (and the depths measured during each campaign).

	2018 (5-95 m depth)			
	Range (median meltrate = 3.45 cm min^{-1})		Median LOD Range Median LOD-	(median meltrate = 4.0
	(5th & 95th percentile t_{10-90} (s)	$\overset{ au_e}{\sim}$	(5th & 95th percentileresolution (cm)	Conductivity (µS en
Dust (# ml ⁻¹) * height Conductivity	97.32 - 707.20 17.5	281.99 <u>8.0</u>	25.00 1.01	-9.8
Ca ²⁺ (ppb) *	-46.4	- 21.1	0.82- 2.71	-57.8
NH ₄ (ppb)	0.07 - 1.03 41.7	0.32-19.0	0.03- 2.39	0.09 - 0.87
H ₂ O ₂ (ppb)	6.84 - 69.92-52.9	26.82 <u>24.1</u>	0.65 -3.04	5.40 - 49.01
Na ⁺ (ppb)	2.39 - 38.89 41.6	13.54 -1 <u>8.9</u>	4.26-2.39	3.01 - 36.41

^{*} Data not included in the published dataset.

5.2 Analytical precision

355

370

The limit of detection (LOD) varies for each detection channel. LOD Sample concentration ranges, LOD, and SD for each of the analytical detection channels are presented in Table 2. LOD is calculated as 3 times the standard deviation of the blank signal measured on ultrapure (MilliQMilliQ®) water during the standard runs (Röthlisberger et al., 2000; Gfeller et al., 2014). Sample concentration ranges and limit of detection (LOD) for each of the analytical detection channels is presented in Table 2The standard deviation (SD) of the lowest concentration standard (9.9 ppb for Ca²⁺ Na⁺, and NH₄ 60 ppb for H₂O₂) is also used as a measure of precision of the system. Frequency histograms for each measured species are presented in Fig. 4.

5.3 Conductivity peak matching

To verify data quality and depth scale accuracy and demonstrate the ability of the CFA record to correlate with signals identified in the discrete dataset, we investigated all conductivity peaks that fall above 3σ from a 90-cm (approximately 3 year) 90 cm moving mean of the conductivity record. The 90 cm window was chosen as on average it represents an approximation of 3 years, despite the known accumulation variability shown in the MBS cores. Using this method, we are able to identify many of the volcanoes-16 of the 32 volcanic events reported in Vance et al. (2024a) (based on the discrete non sea-salt sulfate record) to within one year age-at-depth uncertainty. Volcanoes identified in this method include Pinatubo (1991), Agung (1963), Tambora (1815), Mount Mélébingóy/Parker Peak (1640), Ruiz (1595), and Samalas (1257), in addition to a number of the unknown peaks identified in MBS (Table A2). Additional This method identifies additional peaks above 3σ exist, however have not been matched to volcanoes identified in Vance et al. (2024a), and may be attributed to factors other than volcanic signals.

We consider the ability of the CFA conductivity signal to identify half of the volcanic events found in the non-sea salt sulfate signal by Vance et al. (2024a) across the MBS record to be an external validation of the CFA depth scale and conductivity record described here. We attribute existence of peaks that are not identified in both datasets to the differences in the datasets

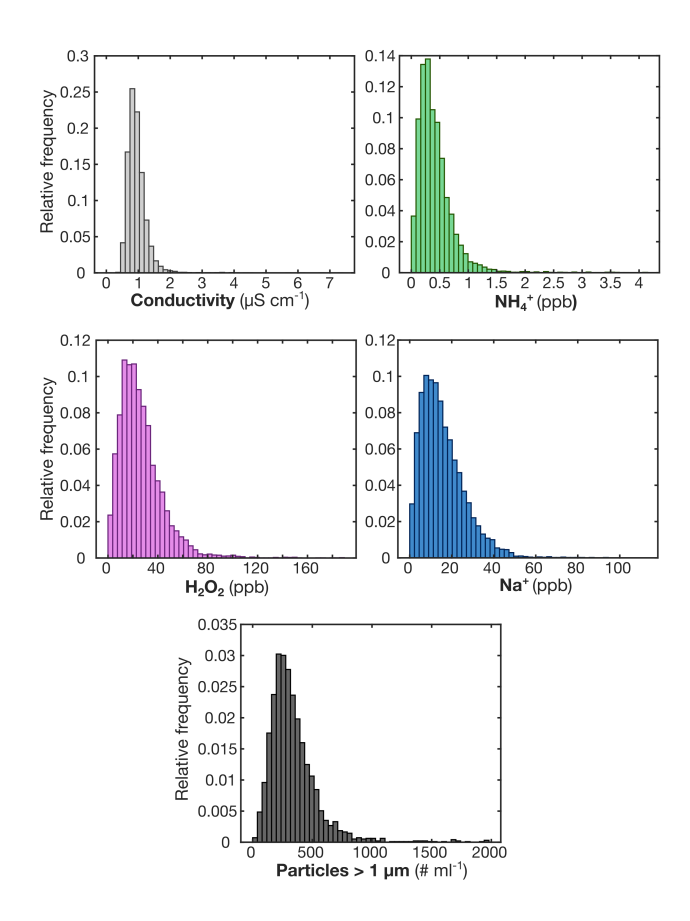


Figure 4. Relative frequency histograms demonstrating the variability of the impurity data (conductivity (μ S cm⁻¹), peroxide (H₂O₂, ppb), sodium (Na⁺, ppb), ammonium (NH₄⁺, ppb), and insoluble microparticles (dust, particles per ml >1 μ m)). Histograms computed based on 3 cm averaged resolution dataset.

used (comparing conductivity to non-sea salt sulfate), as it is likely that some peaks in the conductivity signal are related to sources of other soluble ions, in addition to volcanic sulfate. Additionally, while we use a simple threshold here of 3σ above the moving mean, Vance et al. (2024a) describe only using deviations in non sea salt sulfate from the background, potentially using a lower deviation threshold value.

5.4 Standards preparation

375

380

Measurement uncertainty for the wet chemistry analyses is driven primarily by uncertainty in standards preparation, due to instrument uncertainty of the microliter pipette (20-200 µl Socorex Acura manual®) and bottle-top dispenser (Dispensette®III 5-50 ml, Brand GmbH). This uncertainty is discussed in Gfeller et al. (2014), and as standards used here were prepared in a similar manner, the uncertainty estimate is less than 10 % (Gfeller et al., 2014; Erhardt et al., 2023).

5.5 Contamination and data cleaning

Despite careful decontamination of the ice samples prior to melting, some cleaning of the data is still necessary. Often, very short-duration, high concentration spikes can be seen in the data signal due to occasional air bubbles passing through the measurement cells in the instruments despite the use of debubbler and gas permeable membranes (accurelAccurel ®) immediately prior to each detector. These particular signals are easily identified and removed from the record by a simple 10 second smoothing, or (as implemented here) applying by using a filter that applies a threshold cutoff to the differential of the signal (due to the characteristics of these features). The passage of air bubbles through the detectors results in a signal which is characterized by a significantly steeper increase (and subsequent decrease) in the signal voltage than anything produced by variability in the ice core sample. Because of this characteristic peak shape, we are able to define for the differential of the dataset, a threshold, values above which we use to define "bubble spikes" in the data, which can be safely removed from the dataset.

Contamination signals at core breaks, due to contamination from drill fluid (Estisol-140) or general laboratory contamination, are also relatively easily removed (Erhardt et al., 2022). This type of contamination is characterized by a steep increase in particle count followed by an exponential decay as the contaminated sample passes through the system. For this record, the data coinciding with signals deemed to be caused by this type of contamination have been manually removed from the dataset.

Due to the very low concentrations in Antarctic ice of all species measured and the sensitivity of instrumentation, some measurements fall very close to or below the limit of detection of the system. Data that fall below baseline values (measured from Milli-Q®water run through the system before and after each run) have been removed from the dataset.

6 Dataset description

385

390

395

400

405

410

We present the CFA records in three formats. First, we present the data at 1 mm resolution (full dataset averaged to 1 mm using the CFA depth registration). Although this is in reality an oversampling of the data with regards to the smoothing inherent in the system, we consider this the full dataset at a minimum resolution allowing reduction of instrument noise. While this is below the true resolution when accounting for signal smoothing, the 1 mm resolution dataset can be helpful in identifying extreme events in the dataset which may be artificially smoothed by the moving mean method used to produce the 3 cm averaged dataset.

We also present the data on 3 cm resolution (3 cm averaged), which is above the effective resolution of the instrument-smoothed data for the majority of the measured species. Due to the While 3 cm resolution is lower resolution than the "true" smoothed resolution of some analytes, we chose this resolution so as to provide a cohesive dataset with all species on the same depth scale. Additionally, due to the large annual layer thickness throughout the full record (0.3 m IE yr⁻¹ mean accumulationwith negligible layer thinning throughout) and minimal layer thinning expected at this site (for the 295 m core depth bottom depth with a bedrock depth of approximately 2000 m), data resolution of 3 cm is able to resolve sub-annual features throughout, as seen also in the 3 cm discrete samples (Crockart et al., 2021; Vance et al., 2024a). Figure 5 shows the full length of the CFA record on 3 cm resolution, while Fig. 6 highlights a 50-year subset of the data to demonstrate the resolution of the 3 cm averaged dataset, plotted on the MBS2023 chronology (Vance et al., 2024b). Finally, for ease of use in climate

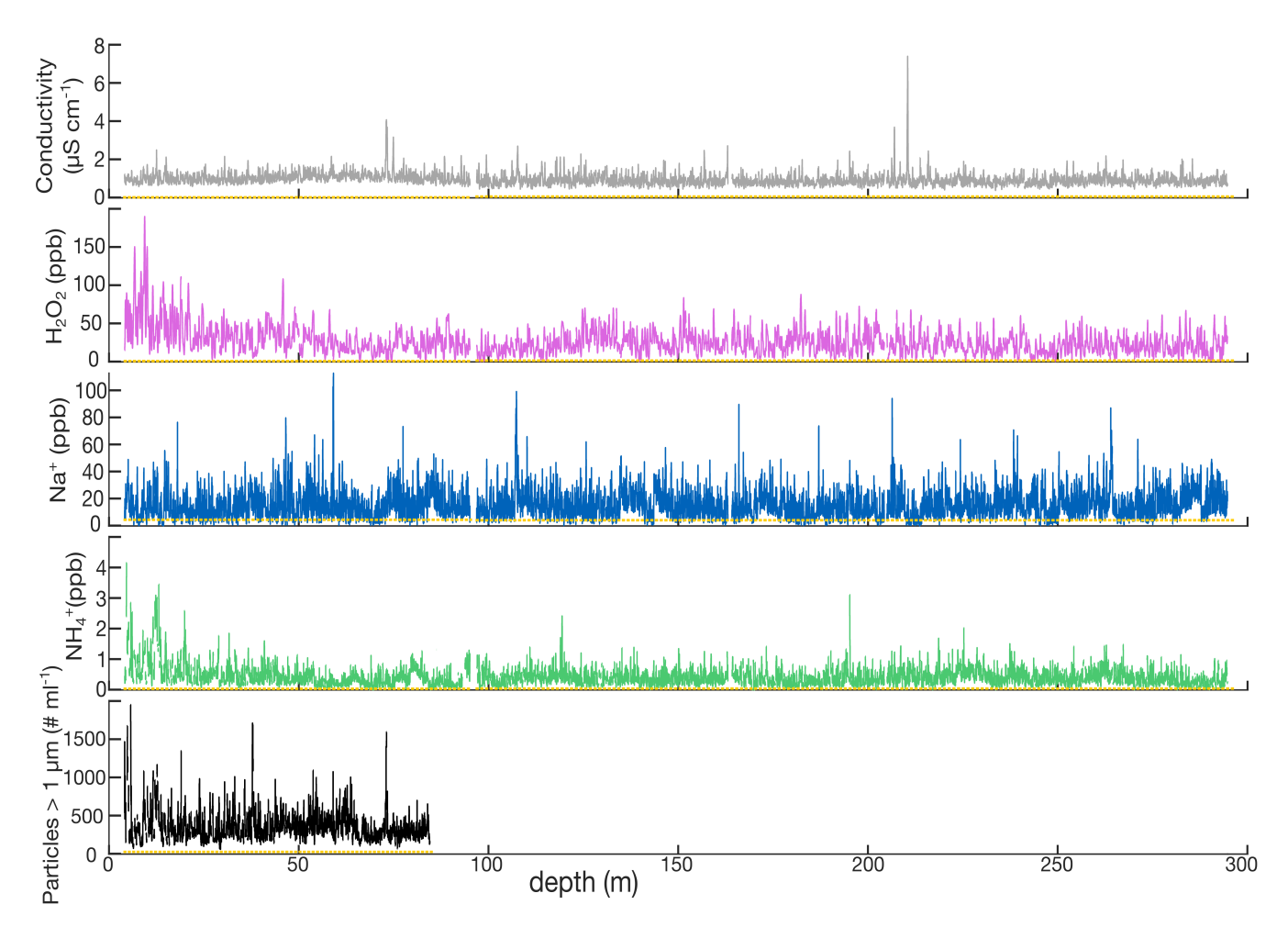


Figure 5. Overview of the full CFA record for MBS at 3 cm resolution. Data include electrolytic conductivity of meltwater (Conductivity, μ S cm⁻¹), peroxide (H₂O₂, ppb), sodium (Na⁺, ppb), (d) ammonium (NH₄⁺, ppb), and (e) insoluble microparticles (dust, particles per ml >1 μ m). Dashed yellow line indicates LOD for each analyte (see Table 2). Gaps in the dataset indicate sections where ice was removed for decontamination, lost in processing, or where analytical issues resulted in poor data quality.

reconstruction application, we present the record as a decadal-scale (10-year) record. The decadal scale record is computed as a 10-year running mean. This is based on the MBS2023 chronology presented in Vance et al. (2024a)), and any future changes in the MBS chronology will not be reflected in this dataset.

Due to the characteristics of accumulation/deposition at the MBS site, care should be taken with interpretation of sub-annual features produced from the 1 mm and 3 cm datasets. We refer readers to Jackson et al. (2023) for a discussion of the impacts of the intermittent precipitation and accumulation variability of the site, and Crockart et al. (2021) for satellite-era climatology and precipitation estimates.

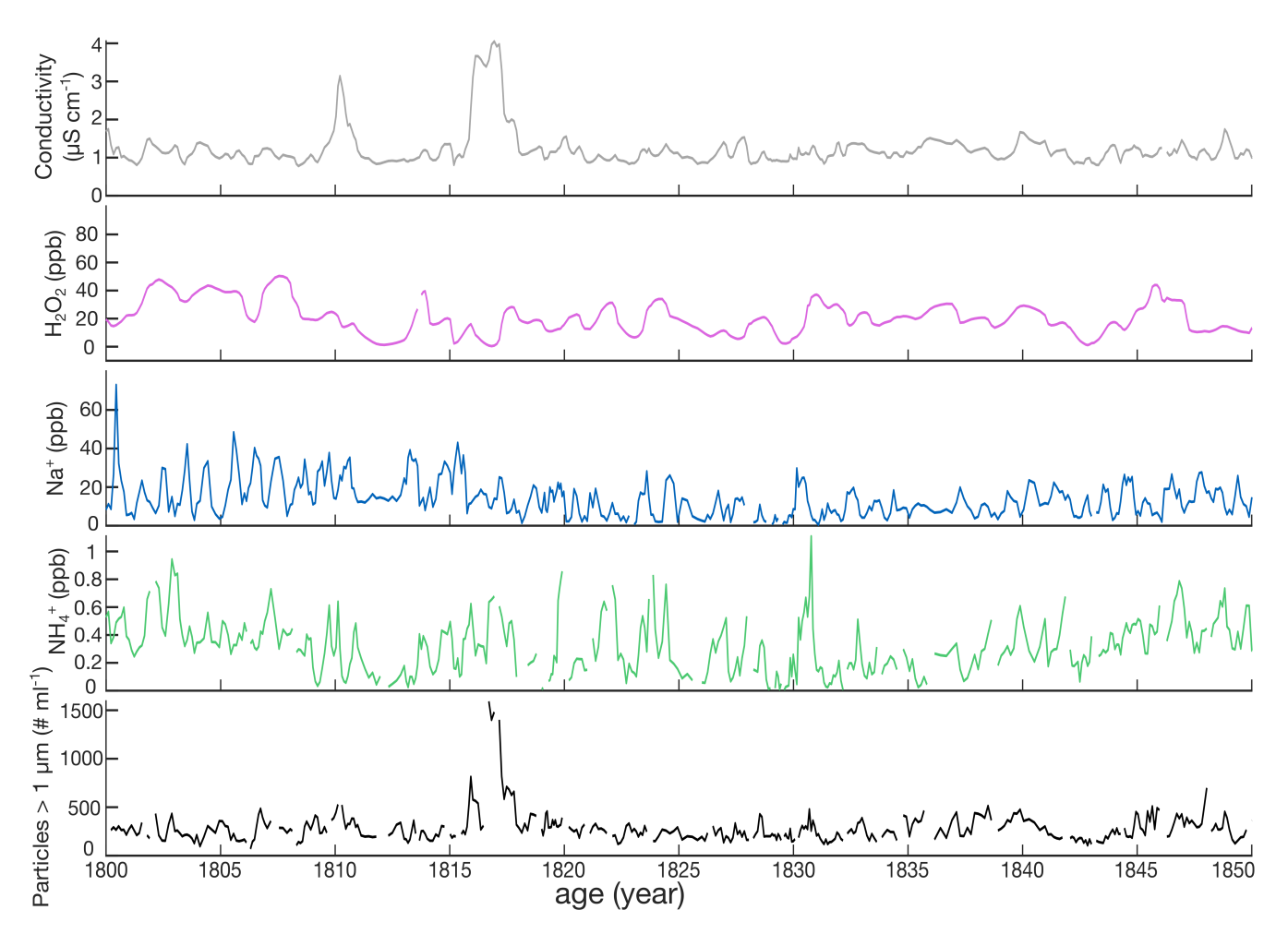


Figure 6. 50 year subset of the 3 cm averaged resolution dataset, covering the period from 1800 to 1850 CE, plotted on the MBS2023 chronology (Vance et al., 2024b). Data shown correspond with the depth range covering approximately 77.55-63.60 m depth of the data presented in Fig. 5. Note the peaks in both conductivity and insoluble microparticles (dust) corresponding with the influence of the 1815 Tambora eruption, one of the volcanic horizons utilized in the development of the MBS2023 chronology (see Fig. A2).

The data datasets presented here (Harlan et al., 2024) has have been cleaned and corrected, both manually and through automated processes. Despite these extensive quality control methods, we cannot guarantee the absence of any spurious data or false signals arising from measurement error or lab contamination.

7 Conclusions

Here we present a high-resolution chemistry and impurity record from the MBS ice core (MBS1718). We present records of electrolytic conductivity, insoluble microparticles (dust), calcium (Ca²⁺), ammonium (NH₄⁺), sodium (Na⁺), and hydrogen

peroxide (H_2O_2) . Based on the chronology presented in Vance et al. (2024a), this record spans 1137 years (873-2009 CE). The data set described here represents the highest resolution chemistry record of the full length of the MBS South-ice core. We are pleased to make this dataset available for public use with considerations to the above comments on resolution and data quality, and the authors remain available for questions by end users.

8 Code availability

430

440

445

The MATLAB scripts described here, used in calibration of the CFA dataset, are available as a supplementary file with this manuscript.

9 Data availability

The datasets described here (1 mm averaged, 3 cm averaged, and decadal averages on the MBS2023 age scale) are available for download from the Australian Antarctic Data Centre (AADC) http://dx.doi.org/doi:10.26179/9tke-0s16 (Harlan et al., 2024).

Author contributions. The Copenhagen CFA system presented here was developed and refined by HAK and Paul Vallelonga. MH, HAK, AdC, TB, VG, SJ, and CP participated in the setup and operation of the CFA system for chemistry, melter, and discrete sample distribution. TRV participated in the MBS1718 ice core drilling. AS, HAK, and AS, CP, and TV participated in freezer work to prepare the ice core. MH, VG, TRV, and SJ constructed the depth scale. MH and AdC conducted the chemistry calibrations with the supervision of HAK. MH and HAK wrote the initial manuscript draft. All authors have reviewed the manuscript and figures and contributed to the finalized manuscript.

Competing interests. The authors declare no competing interests.

Acknowledgements. We would like to acknowledge significant contributions from Paul Vallelonga. The authors would like to thank all participants in the 2018 and 2019 CFA campaigns, including, but not limited to Marius Simonsen, Alexander Zhuravlev, Mirjam Laderach, Nicholas Robles, Estelle Ngoumtsa, Michelle Shu-Ting Lee, Janani Venkatesh, Danielle Udy, Zurine Yoldi, Jia-mei Lin, Anna-Marie Klüssendorf, Andrew Moy, Andy Menking, Todd Sowers, Christo Buziert, Jesper Liisberg, and David Soestmeyer. The Mount Brown South ice core project is led by Tessa Vance, and would not be possible without the team of scientists, technicians, and ice core drillers, including Paul Vallelonga, Jason Roberts, Nerilie Abram, Meredith Nation, Chelsea Long and Alison Criscitiello.

This work was supported by the Australian Government's Antarctic Science Collaboration Initiative (ASCI000002) through funding to the Australian Antarctic Program Partnership. This work contributes to Australian Research Council Discovery Project no. DP220100606. Support for logistics and analytical funding for MBS comes from an Australian Antarctic Science grant (AAS 4414), the Australian Antarctic Division, the Carlsberg Foundation, and a European Union Horizon 2020 research and innovation grant (TiPES, H2020 grant no. 820970). HAK is supported by funding from the Novo Nordic Foundation (PRECISE), the Danish Research Foundation (1131-00007B) and H2020

(820970, 101184070). VG is supported by funding from the Villum Foundation (Villum Fonden Grant 00022995, 00028061) and the Danish Research Foundation (Grant 10.46540/2032-00228B).

Appendix A: Supplementary tables

Table A1. Recipes used in standard solutions. Standards concentrations used are shown in bold.

	Standard Stock (μl)	Milli-Q water (ml)	Concentration (ppb)
Multielement (Ca ² +, NH ₄ ⁺ , and Na ⁺)			
Stock solution	-	-	10^{5}
Std 1 (first dilution)	20	200	9.9
Std 2 (first dilution)	50	200	24.6
Std 3 (first dilution)	200	200	98.5
$\mathbf{H}_{2}\mathbf{O}_{2}$			
Stock solution	-	-	$3x10^{8}$
First dilution	30	100	$9x10^{4}$
Std 1 (second dilution)	100	75	120.0
Std 2 (second dilution)	50	75	60.0

Table A2. Proposed eruption events seen in MBS from Vance et al. (2024a). Events matched with CFA conductivity peaks identified as more than 3 sigma above the 3 year mean. Vance et al. (2024a) depths identified using estimation of the non-sea-salt component of the sulfate from the discrete ion chromatography measurements performed at the Institute for Marine and Antarctic Studies in Hobart, Tasmania, Australia. Dates provided are the volcanic horizons used in development of the MBS2023 chronology (Vance et al., 2024b).

Proposed Event	MBS Depth (m)	Year	CFA conductivity peak depth (m)
		(MBS2023)	(this study)
Pinatubo	12.50	1992.9	12.55
Agung	25.39	1965.1	25.39
Krakatoa	53.96	1885.0	-
Makian	59.67	1864.0	-
Cosiguina	67.39	1837.0	-
Unknown	68.55	1832.0	-
Galunggung	70.91	1824.3	-
Tambora	73.24	1816.3	73.24
Unknown	74.88	1810.3	74.94
Unknown	86.49	1763.2	86.35
Unknown	104.32	1695.9	-
Gamkonora	109.15	1675.0	-
Unknown	114.09	1655.5	114.09
Parker Peak	117.83	1642.4	117.67
Unknown	123.72	1621.1	124.37*
Huaynaputina	129.24	1601.6	-
Ruiz	131.15	1596.0	131.21
Kuwae	162.96	1459.4	162.96
Unknown	180.79	1390.0	-
Unknown	182.58	1382.1	182.59
Unknown	192.02	1345.8	192.09
Unknown	205.02	1287.3	-
Unknown	206.88	1277.5	207.07
Unknown	208.46	1269.5	-
Samalas	210.46	1258.3	210.46
Unknown	213.58	1241.9	-
Unknown	215.64	1230.8	215.94
Unknown	223.55	1192.0	-
Unknown	227.58	1172.3	-
Unknown	240.23	1110.2	240.68*
Unknown	246.36	1082.2	-
Unknown	255.58	1040.6	-

^{*} conductivity peaks with depths close to identified eruption depths in MBS, but not within 30 cm (\sim 1 year).

References

- Agosta, C., Amory, C., Kittel, C., Orsi, A., Favier, V., Gallée, H., van den Broeke, M. R., Lenaerts, J. T. M., van Wessem, J. M., van de Berg, W. J., and Fettweis, X.: Estimation of the Antarctic surface mass balance using the regional climate model MAR (1979–2015) and identification of dominant processes, The Cryosphere, 13, 281–296, https://doi.org/10.5194/tc-13-281-2019, 2019.
 - Bigler, M., Svensson, A., Kettner, E., Vallelonga, P., Nielsen, M. E., and Steffensen, J. P.: Optimization of high-resolution continuous flow analysis for transient climate signals in ice cores, Environmental Science & Technology, 45, 4483–4489, https://doi.org/10.1021/es200118j, 2011.
- Breton, D. J., Koffman, B. G., Kurbatov, A. V., Kreutz, K. J., and Hamilton, G. S.: Quantifying Signal Dispersion in a Hybrid Ice Core

 Melting System, Environmental Science & Technology, 46, 11 922–11 928, https://doi.org/10.1021/es302041k, pMID: 23050603, 2012.
 - Crockart, C. K., Vance, T. R., Fraser, A. D., Abram, N. J., Criscitiello, A. S., Curran, M. A. J., Favier, V., Gallant, A. J. E., Kittel, C., Kjær, H. A., Klekociuk, A. R., Jong, L. M., Moy, A. D., Plummer, C. T., Vallelonga, P. T., Wille, J., and Zhang, L.: El Niño–Southern Oscillation signal in a new East Antarctic ice core, Mount Brown South, Climate of the Past, 17, 1795–1818, https://doi.org/10.5194/cp-17-1795-2021, 2021.
- Dallmayr, R., Goto-Azuma, K., Kjær, H., Azuma, N., TAKATA, M., SCHÜPBACH, S., and Hirabayashi, M.: A High-Resolution Continuous Flow Analysis System for Polar Ice Cores, Bulletin of Glaciological Research, 34, 11–20, https://doi.org/10.5331/bgr.16R03, 2016.
 - Erhardt, T., Bigler, M., Federer, U., Gfeller, G., Leuenberger, D., Stowasser, O., Röthlisberger, R., Schüpbach, S., Ruth, U., Twarloh, B., Wegner, A., Goto-Azuma, K., Kuramoto, T., Kjær, H. A., Vallelonga, P. T., Siggaard-Andersen, M.-L., Hansson, M. E., Benton, A. K., Fleet, L. G., Mulvaney, R., Thomas, E. R., Abram, N., Stocker, T. F., and Fischer, H.: High-resolution aerosol concentration data from the
- Greenland NorthGRIP and NEEM deep ice cores, Earth System Science Data, 14, 1215–1231, https://doi.org/10.5194/essd-14-1215-2022, 2022.
 - Erhardt, T., Jensen, C. M., Adolphi, F., Kjær, H. A., Dallmayr, R., Twarloh, B., Behrens, M., Hirabayashi, M., Fukuda, K., Ogata, J., Burgay, F., Scoto, F., Crotti, I., Spagnesi, A., Maffezzoli, N., Segato, D., Paleari, C., Mekhaldi, F., Muscheler, R., Darfeuil, S., and Fischer, H.: High resolution aerosol data from the top 3.8 ka of the EGRIP ice core, Earth System Science Data Discussions, 2023, 1–21, https://doi.org/10.5194/essd-2023-176, 2023.
 - Foster, A. F., Curran, M. A., Smith, B. T., Van Ommen, T. D., and Morgan, V. I.: Covariation of Sea ice and methanesulphonic acid in Wilhelm II Land, East Antarctica, Annals of Glaciology, 44, 429–432, https://doi.org/10.3189/172756406781811394, 2006.
 - Gfeller, G., Fischer, H., Bigler, M., Schüpbach, S., Leuenberger, D., and Mini, O.: Representativeness and seasonality of major ion records derived from NEEM firn cores, The Cryosphere, 8, 1855–1870, https://doi.org/10.5194/tc-8-1855-2014, 2014.
- Gkinis, V., Popp, T. J., Blunier, T., Bigler, M., Schüpbach, S., Kettner, E., and Johnsen, S. J.: Water isotopic ratios from a continuously melted ice core sample, Atmospheric Measurement Techniques, 4, 2531–2542, https://doi.org/10.5194/amt-4-2531-2011, 2011.
 - Gkinis, V., Jackson, S., Abram, N. J., Curran, M., Blunier, T., Halan, M., Kjær, H. A., Moy, A., Peensoo, K., Quistgaard, T., Vance, T. R., and Vallelonga, P.: An 1135 year very high-resolution water isotope record of polar precipitation from the Indo-Pacific sector of East Antarctica, Ver. 1, Australian Antarctic Data Centre, https://doi.org/doi:10.26179/ygeq-1a95, accessed: 2024-09-07, 2024a.
- 490 Gkinis, V., Jackson, S., Abram, N. J., Plummer, C., Blunier, T., Harlan, M. M., Kjær, H. A., Moy, A. D., Peensoo, K. M., Quistgaard, T., Svensson, A., and Vance, T. R.: An East Antarctic, sub-annual resolution water isotope record from the Mount Brown South Ice core, Nature Scientific Data, 11, https://doi.org/10.1038/s41597-024-03751-w, 2024b.

- Harlan, M., Kjær, H. A., Vance, T., Gkinis, V., Jackson, S., Blunier, T., Svensson, A., Plummer, C., de Campo, A., and Vallelonga, P.: 1137 years of high-resolution Continuous Flow Analysis impurity data from the Mount Brown South Ice Core, Ver. 1, Australian Antarctic Data

 Centre, https://doi.org/doi:10.26179/9tke-0s16, accessed: 2024-08-02, 2024.
 - Jackson, S. L., Vance, T. R., Crockart, C., Moy, A., Plummer, C., and Abram, N. J.: Climatology of the Mount Brown South ice core site in East Antarctica: implications for the interpretation of a water isotope record, Climate of the Past, 19, 1653–1675, https://doi.org/10.5194/cp-19-1653-2023, 2023.
- Jones, T. R., White, J. W. C., Steig, E. J., Vaughn, B. H., Morris, V., Gkinis, V., Markle, B. R., and Schoenemann, S. W.: Improved methodologies for continuous-flow analysis of stable water isotopes in ice cores, Atmospheric Measurement Techniques, 10, 617–632, https://doi.org/10.5194/amt-10-617-2017, 2017.
 - Kaufmann, P., Federer, U., Hutterli, M. A., Bigler, M., Schüpbach, S., Ruth, U., Schmitt, J., and Stocker, T. F.: An improved continuous flow analysis system for high-resolution field measurements on ice cores, Environmental Science & Technology, 42, 8044–8050, https://doi.org/10.1021/es8007722, 2008.
- Kjær, H. A., Zens, P., Black, S., Lund, K. H., Svensson, A., and Vallelonga, P.: Canadian forest fires, Icelandic volcanoes and increased local dust observed in six shallow Greenland firn cores, Climate of the Past, 18, 2211–2230, https://doi.org/10.5194/cp-18-2211-2022, 2022.
 - Kjær, H. A., Vallelonga, P., Svensson, A., Elleskov L. Kristensen, M., Tibuleac, C., Winstrup, M., and Kipfstuhl, S.: An Optical Dye Method for Continuous Determination of Acidity in Ice Cores, Environmental Science & Technology, 50, 10485–10493, https://doi.org/10.1021/acs.est.6b00026, pMID: 27580680, 2016.
- Kjær, H. A., Hauge, L. L., Simonsen, M., Yoldi, Z., Koldtoft, I., Hörhold, M., Freitag, J., Kipfstuhl, S., Svensson, A., and Vallelonga, P.: A portable lightweight in situ analysis (LISA) box for ice and snow analysis, The Cryosphere, 15, 3719–3730, https://doi.org/10.5194/tc-15-3719-2021, 2021.
 - Legrand, M. and Mayewski, P.: Glaciochemistry of polar ice cores: A review, Reviews of Geophysics, 35, 219–243, https://doi.org/https://doi.org/10.1029/96RG03527, 1997.
- Rhodes, R. H., Faen, X., Stowasser, C., Blunier, T., Chappellaz, J., McConnell, J. R., Romanini, D., Mitchell, L. E., and Brook, E. J.: Continuous methane measurements from a late Holocene Greenland ice core: Atmospheric and in-situ signals, Earth and Planetary Science Letters, 368, 9–19–9–19, http://www.sciencedirect.com/science/article/pii/S0012821X13001088, 2013.

520

- Röthlisberger, R., Bigler, M., Hutterli, M., Sommer, S., Stauffer, B., Junghans, H. G., and Wagenbach, D.: Technique for continuous high-resolution analysis of trace substances in firn and ice cores, Environmental Science & Technology, 34, 338–342, https://doi.org/10.1021/es9907055, 2000.
- Sigg, A., Fuhrer, K., Anklin, M., Staffelbach, T., and Zurmuehle, D.: A continuous analysis technique for trace species in ice cores, Environmental Science & Technology, 28, 204–209, https://doi.org/10.1021/es00051a004, doi: 10.1021/es00051a004, 1994.
- Simonsen, M., Baccolo, G., Blunier, T., Borunda, A., Delmonte, B., Frei, R., Goldstein, S., Grinsted, A., Kjær, H. A., Sowers, T., Svensson, A., Vinther, B., Vladimirova, D., Winckler, G., Winstrup, M., and Vallelonga, P.: East Greenland ice core dust record reveals timing of Greenland ice sheet advance and retreat, Nature Communications, 10, https://doi.org/10.1038/s41467-019-12546-2, 2019.
- Simonsen, M. F., Cremonesi, L., Baccolo, G., Bosch, S., Delmonte, B., Erhardt, T., Kjær, H. A., Potenza, M., Svensson, A., and Vallelonga, P.: Particle shape accounts for instrumental discrepancy in ice core dust size distributions, Climate of the Past, 14, 601–608, https://doi.org/10.5194/cp-14-601-2018, 2018.
- Smith, B. T., van Ommen, T. D., and Morgan, V. I.: Distribution of oxygen isotope ratios and snow accumulation rates in Wilhelm II Land,
 East Antarctica, Annals of Glaciology, 35, 107–110, https://doi.org/10.3189/172756402781816898, 2002.

- Stowasser, C., Buizert, C., Gkinis, V., Chappellaz, J., Schüpbach, S., Bigler, M., Faïn, X., Sperlich, P., Baumgartner, M., Schilt, A., and Blunier, T.: Continuous measurements of methane mixing ratios from ice cores, Atmos. Meas. Tech. Techniques, 5, 999–1013–999–1013, https://doi.org/10.5194/amt-5-999-2012, 2012.
- Vance, T. R., Roberts, J. L., Moy, A. D., Curran, M. A., Tozer, C. R., Gallant, A. J., Abram, N. J., Ommen, T. D. V., Young, D. A., Grima,
 C., Blankenship, D. D., and Siegert, M. J.: Optimal site selection for a high-resolution ice core record in East Antarctica, Climate of the Past, 12, 595–610, https://doi.org/10.5194/cp-12-595-2016, 2016.
 - Vance, T. R., Abram, N. J., Criscitiello, A. S., Crockart, C. K., DeCampo, A., Favier, V., Gkinis, V., Harlan, M., Jackson, S. L., Kjær, H. A., Long, C. A., Nation, M. K., Plummer, C. T., Segato, D., Spolaor, A., and Vallelonga, P. T.: An annually resolved chronology for the Mount Brown South ice cores, East Antarctica, Climate of the Past, 20, 969–990, https://doi.org/10.5194/cp-20-969-2024, 2024a.
- Vance, T. R., Abram, N. J., Gkinis, V., Harlan, M., Jackson, S., Plummer, C., Segato, D., Spolaor, A., Vallelonga, P., Nation, M. K., Long, C., and Kjær, H. A.: MBS2023 The Mount Brown South ice core chronologies and chemistry data, Ver. 1, Australian Antarctic Data Centre, https://doi.org/doi:10.26179/352b-6298, accessed: 2024-09-07, 2024b.